University of Alberta

The study of claudins in a model system of the proximal tubule

by

Jelena Borovac

A thesis submitted to the Faculty of Graduate Studies and Research
in partial fulfillment of the requirements for the degree of

Master of Science

Department of Physiology

Spring 2013
Edmonton, Alberta

ABSTRACT

The proximal tubule (PT) is a major site of paracellular transport. Research in this area is undermined by the lack of a model system that is representative of PT electrophysiology. We examined opossum kidney (OK) cell characteristics and found a striking resemblance to the PT (transepithelial resistance = 11.7 Ω cm^2 and the permeability ratio P_{Na+}/P_{Cl-} = 1.08). Furthermore, OK cells express a number of claudins (claudin-4 > -1 > -6 > -20 > -9 > -12 > -11 > -15, in order of the amount of expression), which are known to regulate paracellular transport. We over-expressed claudin-2 and found that it forms a non-selective pore at the tight junction of OK cells. Over-expression of claudin-4, on the other hand, led to the formation of a non-selective barrier. However, the expression of these isoforms caused significant perturbations in expression of endogenous claudins leading us to conclude that claudin expression is strongly interdependent.

ACKNOWLEDGEMENTS

I would like to thank Dr. Todd Alexander for giving me the opportunity to partake in this wonderful project. His incredible patience, knowledge and enthusiasm kept me motivated and excited about my experiments. Through all the ups and downs of my research, I could not have asked for a better mentor. I would also like to thank my mom Radojka and sister Snjezana for all their love, support and understanding.

I have a great appreciation for the hard work of our summer students: Reid Barker who performed the initial experiments involving OK/claudin-4 qRT-PCR and Ussing Chambers and Andrew Rasmussen who helped with OK cell molecular characterization. I owe a special thanks to Dr. Marek Duszyk and Dr. Juraj Rievaj for their patience and support while teaching me the Ussing Chamber protocols. Along with Juraj, I was proud to work with some wonderful colleagues and friends- Devishree Krishnan, Prajakta Desai and Wanling Pan. This project would not be possible without the help of Wanling, who taught and encouraged me since my very first day at the lab. For all the insightful advice and guidance, I would like to thank our lab meeting colleagues Dr. Cordat & Lab, as well as my Committee Members Dr. Wevrick and Dr. Chen. Last, but not least, I would like to thank the Kidney Foundation of Canada for their financial support in this project.

TABLE OF CONTENTS

Chapter 1: INTRODUCTION 1
1.1 The kidney 2
1.2 Proximal tubule 3
1.2.1 Ion and water transport 3
1.2.2 Resistance and permeability characteristics 3
1.3 Paracellular versus transcellular transport 4
1.4 Claudins 5
1.4.1 Claudin structure and function 5
1.4.2 Claudins and transepithelial resistance 7
1.4.3 Cation and anion selective Claudins 8
1.4.4 Regulatory mechanisms 10
1.4.5 Claudin interactions 11
1.4.6 Claudins in the proximal tubule 13
1.5 Common model systems for studying Claudins 14
1.5.1 MDCK cells 14
1.5.2 LLC-PK1 cells 15
1.5.3 Importance of the model system characteristics 16
1.6 OK cells 18
1.7 Hypothesis 18
1.8 Objectives 18

Chapter 2: MATERIALS AND METHODS 19
2.1 Cell culture and stable cell lines 20
2.2 Antibodies 20

2.3 Molecular Biology 21
2.3.1 Expression PCR 21
2.3.2 Cloning and plasmid construction 21
2.3.3 Quantitative Real-time PCR 26
2.3.4 siRNA knockdown 28
2.4 Expression and Localization studies 29
2.4.1 Immunoblot analysis 29
2.4.2 Immunohistochemistry 29
2.5 Functional studies 30
2.5.1 Ussing Chamber Experiments 30
2.5.2 Fluorescent Dextran Flux 33
2.6 Statistical analysis 33

Chapter 3: RESULTS 34
3.1 OK cells 35
3.1.1 OK cells form a tight junction 35
3.1.2 Tight junction characteristics 35
3.2 Claudins in OK cells 40
3.2.1 Claudins expressed 40
3.2.2 Relative claudin expression 42
3.3 Claudin 2 42
3.3.1 Expression and stable cell lines 42
3.3.2 Effects on paracellular permeability 45
3.3.3 Claudin-2 expression alters endogenous claudin levels 45
3.4 Claudin 4 48
3.4.1 Expression and stable cell lines 48
3.4.2 Effects on electrophysiology 48
3.4.3 Paracellular flux of fluorescent dextrans 52
3.4.4 Effects on endogenous claudins 52
3.4.5 Claudin-4 siRNA knockdown 55

Chapter 4: DISCUSSION 60
4.1 Opossum kidney cells as a model system of the proximal tubule ... 61
4.1.1 Electrophysiology 61
4.1.2 Claudins 62
4.2 Claudin 2 in OK cells 63
4.3 Claudin 4 in OK cells 64
4.3.1 Claudin-4 over-expression 64
4.3.2 Effects on endogenous claudins 66
4.3.3 Claudin-4 knockdown 67
Summary 70
Conclusion 72
Future directions 72
Bibliography 73

LIST OF TABLES

Table 1.1 Properties of Claudin-2 and Claudin-4 9
Table 2.1 Claudin PCR primers 22
Table 2.2: Claudin Cloning Primers 25
Table 2.3 Claudin qRT-PCR primers and probes 27

LIST OF FIGURES

Figure 1.1 Claudin structure..... 6
Figure 1.2 Claudin interactions..... 12
Figure 2.1 Ussing Chamber Dilution Potentials 32
Figure 3.1 OK cell tight junction 36
Figure 3.2 OK, MDCK II and LLC-PK1 tight junction electrophysiology..... 37
Figure 3.3 Permeability profile of the OK cell tight junction..... 39
Figure 3.4 Claudin expression in OK cells 41
Figure 3.5 Relative claudin expression 43
Figure 3.6 Expression of mouse claudin 2 in OK cells..... 44
Figure 3. 7 Effects of claudin 2 expression on electrophysiology 46
Figure 3.8 Effects of claudin 2 on endogenous claudins in OK cells 47
Figure 3.9 Claudin-4 sequence..... 49
Figure 3.10 Claudin 4 expression 50
Figure 3.11 Effects of claudin 4 expression on OK cell electrophysiology 51
Figure 3.12 Claudin 4 effects on paracellular dextran permeability..... 53
Figure 3.13 Claudin 4 – effects on endogenous claudins 54
Figure 3.14 Claudin 4 knockdown..... 56
Figure 3.15 Claudin 4 knockdown- effects on endogenous claudins 58
Figure 3.16 OK claudin 4 knockdown- effects on electrophysiology 59

LIST OF ABBREVIATIONS

Abbreviation	Meaning
CD	collecting duct
Cldn	claudin
DCT	distal convoluted tubule
ECL	extracellular loop
IF	immunofluorescence
LOH	loop of henle
PCT	proximal convoluted tubule
pNa^+/pCl^-	permeability ratio
PST	proximal straight tubule
PT	proximal tubule
TER	transepithelial resistance
TJ	tight junction
WB	western blot
ZO-1	zonula occludens protein 1

Model system abbreviations

Abbreviation	Cell type
HEK293	human embryonic kidney 293
HK	human kidney cells
HRPTE	human renal proximal tubule epithelial cells
LLCPK	pig kidney epithelial cells
MDCK	Madin Darby canine kidney
NRK-52E	rat kidney epithelial cells
OK	opossum kidney cells

CHAPTER 1

INTRODUCTION

1. INTRODUCTION

1.1 The kidney

The kidney is central to the processes of maintaining ion homeostasis, pH and blood volume. These delicate balances are achieved by the sophisticated regulation of transport pathways localized along the segments of the nephron (functional unit of the kidney). The kidney is made up of about a million nephron units each consisting of a bulbous filtration structure, the glomerulus, which filters blood into the remaining tubular segments: Proximal Convoluted Tubule (PCT), proximal straight tubule (PST) and Loop of Henle (LOH), which itself consists of the Thin Descending Limb, Thin Ascending Limb and the Thick Ascending Limb. The LOH continues into the Distal Convoluted Tubule (DCT), Connecting tubule (CNT) and the Collecting Duct (CD). The glomerulus carries out the first step, simple filtration, which allows for plasma solutes, except proteins greater than approximately 60 kDa, to enter the lumen of the nephron. The role of the remaining segments is the reabsorption of ions and water. The efficiency of NaCl and water reabsorption is so vast that out of 180L filtered/day only about 1% is excreted. The large majority of water, Na^+, Cl^- and other ions are reabsorbed across the proximal tubule epithelium, as discussed in detail below. The next 20-25% of NaCl and 15% of water are reabsorbed from Henle's Loop and the remainder from the Distal Tubule, Connecting Tubule and the Collecting Duct. These late segments are also known as the 'aldosterone sensitive distal nephron' (ASDN) because they are regulated by the sodium retention hormone aldosterone. Altogether, the ASDN reabsorbs a small percentage of ions to achieve the

necessary fine adjustments in final ion concentration (56). Unlike the distal segments, the proximal tubule is the site of copious water and ion reabsorption, specifically 110 L of water and 1.6 kg of NaCl per day.

1.2 Proximal tubule

1.2.1 Ion and water transport

The proximal tubule can be further subdivided into three distinct segments, which differ morphologically. S1 is the first convoluted portion. It is followed by S2, which is convoluted at first and then straight. S3 is the entirely straight portion of the tubule located furthest from the glomerulus (32). The earlier segments house a greater number of mitochondria and exhibit higher transport capacity (65). The proximal tubule is a major site of ion retrieval, with 80-90% of the filtered phosphate (76), ~65% of sodium (31), 50-60% of chloride (91), 65% of potassium (41), ~80% of filtered bicarbonate (16) and up to 70% of calcium (42) being reabsorbed there. The majority of water reabsorption, ~60% (26), also occurs across the proximal tubule. Experiments using rabbit proximal tubule perfusion techniques by Capri-Medina and Whittembury suggest that about 50% of the water reabsorption from the PT occurs strictly by paracellular mechanisms, which are described in detail below (20). In order to accommodate such high flux rates, the proximal tubule has unique resistance and permeability characteristics compared to other epithelia in the body.

1.2.2 Resistance and permeability characteristics

The proximal tubule epithelium has very low transepithelial resistance (TER). A resistance value between 5 and 12 Ω cm^2 is commonly reported for the dog,

rabbit, rat and mouse proximal tubule epithelia (14, 17, 64, 77, 88, 93). This value is incredibly low, especially when it is compared to epithelia such as the urinary bladder, which can reach a TER as high as 300 000 Ω cm^2 (62). The low resistance of the proximal tubule is consistent with significant permeability to water and ions. The relative transepithelial fluxes of sodium and chloride can be translated into a pNa^+/pCl^- ratio, the term used to describe perm-selectivity of an epithelium. A pNa^+/pCl^- ratio greater than 1 indicates a cation selective epithelium, whereas epithelia with pNa^+/pCl^- lower than 1 are anion selective. The proximal tubule is slightly cation selective, with pNa^+/pCl^- of 1.38 reported in dog (17), 1.58 in rat (73) and 1.10 in mouse (77) proximal tubule studies. Only one study reports anion selectivity in rat proximal tubule, with a pNa^+/pCl^- ratio of 0.75 (13). This type of variability could result if a different segment of the proximal tubule was isolated for the latter experiment (*i.e.* S1 *vs* S2).

Much of the ion and water reabsorption at the proximal tubule occurs by passive mechanisms. Passive reabsorption refers largely to paracellular processes, which are not as well understood as transcellular processes. Paracellular transport also occurs in the Loop of Henle, while the distal portions of the nephron have a much higher resistance and exhibit almost entirely transcellular transport (109).

1.3 Paracellular versus transcellular transport

Transcellular transport refers to the movement of molecules across an epithelium through cells. This necessitates the crossing of at least two membranes. To achieve this, the participation of ion channels, membrane transporters and cytoplasmic carriers is almost always needed. Paracellular transport, on the other

hand, is the movement of molecules across the epithelium through the tight junction, the most apical intercellular junctional complex (94). Various techniques are used to study paracellular transport, including permeability assays with radioactively labeled tracers (*i.e.* mannitol) and fluorescent dextran molecules (7, 93, 99, 110). The study of specific paracellular ion permeability can also be performed using radiolabeled molecules, but Ussing Chamber dilution potential measurements are preferred (44, 73, 104). Paracellular transport is controlled by the presence and distribution of tight junction molecules called claudins.

1.4 Claudins

1.4.1 Claudin structure and function

Claudins are small proteins, ranging from ~20-27 kDa molecular weight, with four transmembrane spanning regions, cytoplasmic amino and carboxy termini and two extracellular loops, which both face the paracellular space (36, 100, 103). The second loop is smaller (~ 20 amino acids), compared to the first loop which is made up of ~50 amino acids (Figure 1.1). Claudins are expressed in epithelial cells including the intestine, blood brain barrier, skin and throughout the nephron. Claudins that exhibit very strong sequence homology have been classified as classic claudins (1 – 10, -14, -15, -17 and -19), while the rest of the isoforms are "non-classic" (11–13, 16, 18, 20–24) (59). The charged amino acid composition of the larger loop correlates with selectivity properties of various claudin isoforms (25), while the second, smaller loop may be important for claudin interactions (80). Claudin function is, therefore, to 'select' the molecules for passage through the tight junction. The presence and distribution of claudins at the tight junction

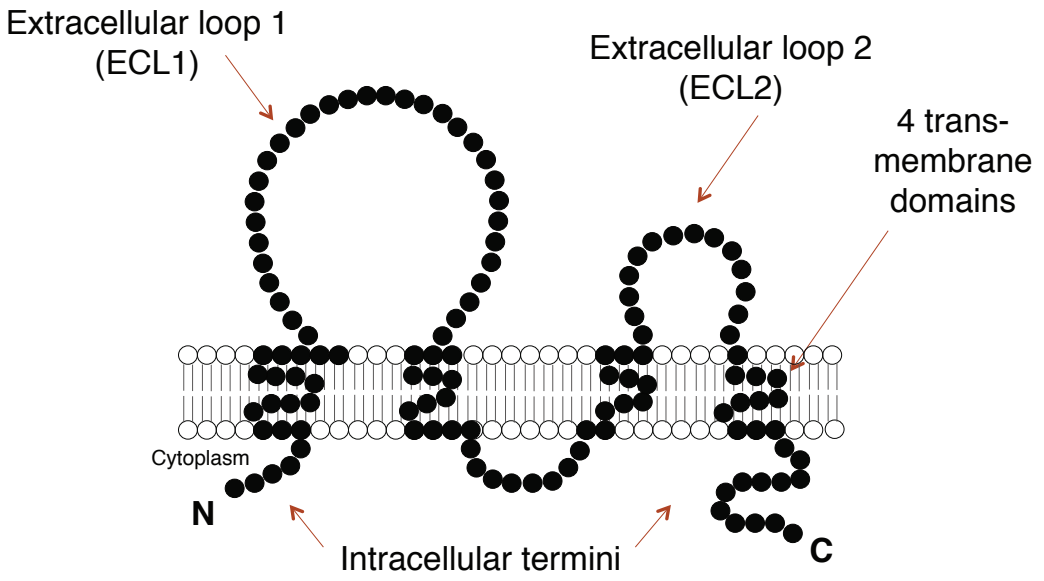

Figure 1.1 *Claudin structure.* Diagrammatic representation of claudin structure: depicting two intracellular termini, 4 transmembrane domains and two extracellular loops (ECL1 and ECL2).

governs the resistance of the paracellular shunt pathway (TER) and the preference to cation or anion flux (*i.e.* pNa^+/pCl^-) (59). More specifically, claudins can be considered: 'anion selective', 'cation selective', 'barrier forming', or 'pore forming', depending on the effect of their over-expression (or removal) on ion permeability and transepithelial resistance (75). Of the 27 mammalian claudin isoforms identified to date (72), very few have been strictly defined as barriers or pores in the tight junction.

1.4.2 Claudins and transepithelial resistance

Claudins assemble into tight junction strands at the "kissing points" between adjacent cells (100). It is now known that claudins can actually reconstitute such strands in fibroblasts, which intrinsically lack tight junctions (39). A weak correlation has been observed between the number of tight junction strands and TER (22, 23). Interestingly, the expression of claudin-4, a protein discussed in detail later, was found to correspond with strand number. Specifically, in MDCK I cells, the removal of claudin-4 resulted in decreased barrier function as well as a decreased number of tight junction strands (96). However, not all claudins form barriers, as evinced by claudin-2, a protein well known for its pore forming properties (4, 35, 37, 85, 104). Although it is agreed that claudin-2 forms a "channel", it is difficult to firmly classify each claudin as barrier- or pore-forming. For instance, it is possible for an anion selective claudin to channel the flux of anions, but at the same time form a barrier to the flux of cations. Experimental results from Hou and colleagues suggest this to be the case with claudin-4 (43).

1.4.3 Cation and anion selective Claudins

The limited data available so far has made it possible to loosely classify claudins -2, -6, -7, -9, -10b, -12, -15 and -16 as cation selective (4, 35, 43, 44, 86, 103, 104) and -4 , -5 , -7 , -8 , -10a , -11, -14, and -19 as anion selective (3, 8, 15, 43, 102, 104, 106, 108, 111). The permselectivity properties of claudin-2 and claudin-4 are summarized in Table 1.1. Charged amino acids of the first extracellular loop (ECL1) correspond with the selectivity properties of claudins. In fact, a linear relationship was found between charge selectivity and the net charge of residues in the second half of the first ECL (specifically amino acids 52-77) (104).

Negative amino acid net charge results in lower anion permeability (and therefore cation selectivity). This is the case with claudin-2. However, if positively charged amino acids outnumber negatively charged ones, like they do with claudin-4, cation flux is repelled and the result is anion selectivity. An elegant study published in 2002 found that charge reversal of amino acids in ECL1 reversed paracellular charge selectivity (25). In this experiment, a mutation of a positive to a negative amino acid in the first ECL of claudin-4 increased cation permeability. Together, the combination of all claudins expressed in the tight junction exerts a permselectivity of the epithelium. As discussed later, the perceived function of claudins highly depends on the properties of the cell line in which they are expressed. The cell lines most commonly used to study claudins are LLC-PK1 and MDCK cells (detailed in section 1.5.1 and 1.5.2). The combination of claudins in LLC-PK1 epithelial cells results in anion selectivity (pNa^+/pCl^- ratio = 0.42 ± 0.04 (82)). MDCK cells, on the other hand, are cation selective with

	CLAUDIN-2	CLAUDIN-4
Effect on TER	Decrease (4, 37)	Increase (102, 104)
Net charge in the first ECL	(-) (24, 104, 112)	(+) (24, 104)
Charge selectivity	(+) (4, 60, 77, 104, 112)	(-) (43, 47, 60, 102)
Function	Cation selective pore	Anion selective barrier

Table 1.1 *The properties of Claudin-2 and Claudin-4*
The summary of permselectivity characteristics available for claudin-2 and -4

pNa^+/pCl^- ratios ranging from 1.7 (73) to 10 (7) depending on the clone. In order to maintain such stable perm-selectivity properties in epithelial model systems and the epithelia of our body, claudin expression must be tightly regulated.

1.4.4 Regulatory mechanisms of claudin expression

As of yet, claudin regulation is a relatively unexplored field. A few transcription factors have been associated with regulation of claudin expression, including GATA-4, an enhancer of intestinal claudin-2 expression (34), T/EBP/NKX2.1 which increases claudin-18 expression in the lung (78), Cdx2 (intestinal and gastric activator of claudin -3 and -4) (87) and Snail (50, 79). Snail is a transcription factor involved in the regulation of epithelial to mesenchymal transition (EMT) (19) as well as cancer development and progression (29). Moreover, Snail was reported to down-regulate claudins -1, -2 -3, -4, and -7, as well as occludin (21, 50, 67, 79) and its activation in the adult kidney is associated with renal fibrosis (18). So far, there is no other information available about transcription factors regulating claudin expression in the kidney. Regulation of claudins at the level of transcription is almost exclusively studied with regards to cancer development and progression.

Claudins are also regulated at the level of trafficking and tight junction incorporation. In fact, the assembly of claudins at the tight junction is not possible without their interaction with ZO-1 and ZO-2, the scaffolding proteins which link claudins to the actin cytoskeleton (101). Regulation of claudins at the tight junction occurs by endocytosis, or more specifically internalization by the unique cell-eat-cell mechanism (68). In this model, a cell can internalize a portion of the

adjacent cell membrane with claudins, while leaving the tight junction intact. Perhaps the most interesting regulator of claudins reported so far is another claudin competing for the tight junction space. Angelow *et. al.* described this phenomenon, following the observation that claudin-8 expression in MDCK II cells decreases claudin-2 gene expression and inhibits claudin-2 trafficking to the tight junction (9). Studies like this certainly endorse the belief that claudins are carefully selected based on their compatibility with other claudins and their ability to interact with neighboring tight junctions.

1.4.5 Claudin interactions

Interactions between different (heterophilic) and the same (homophilic) claudin isoform may occur within the cell membrane (*cis*) or across the paracellular space with claudins of the adjacent membrane (*trans*) (40) (Figure 1.2). Homophilic *cis* interaction, or formation of claudin oligomers has been described for claudin-4 and claudin-5 (27, 74). Perhaps more interesting is the interaction between claudins of adjacent cells across the paracellular space, or *trans*-interaction. Homophilic *trans* interaction occurs for claudin-1, -2, -3, -5, -6, -9, -11, -14, and -19 (59). The number of claudins reported to demonstrate heterophilic *trans*-interactions is much lower. In fact, interactions between claudins -1 and -3, -2 and -3 and -5 and -3 are the only cases reported so far (27, 40). Finally, heterophilic *cis* interaction was described for claudin -2 and -3 (40), claudin 3- and -4 (28) and claudin -16 and -19 (45). Despite their ability to interact within the same membrane, claudin -3 and -4 cannot undergo *trans* –interaction. This phenomenon

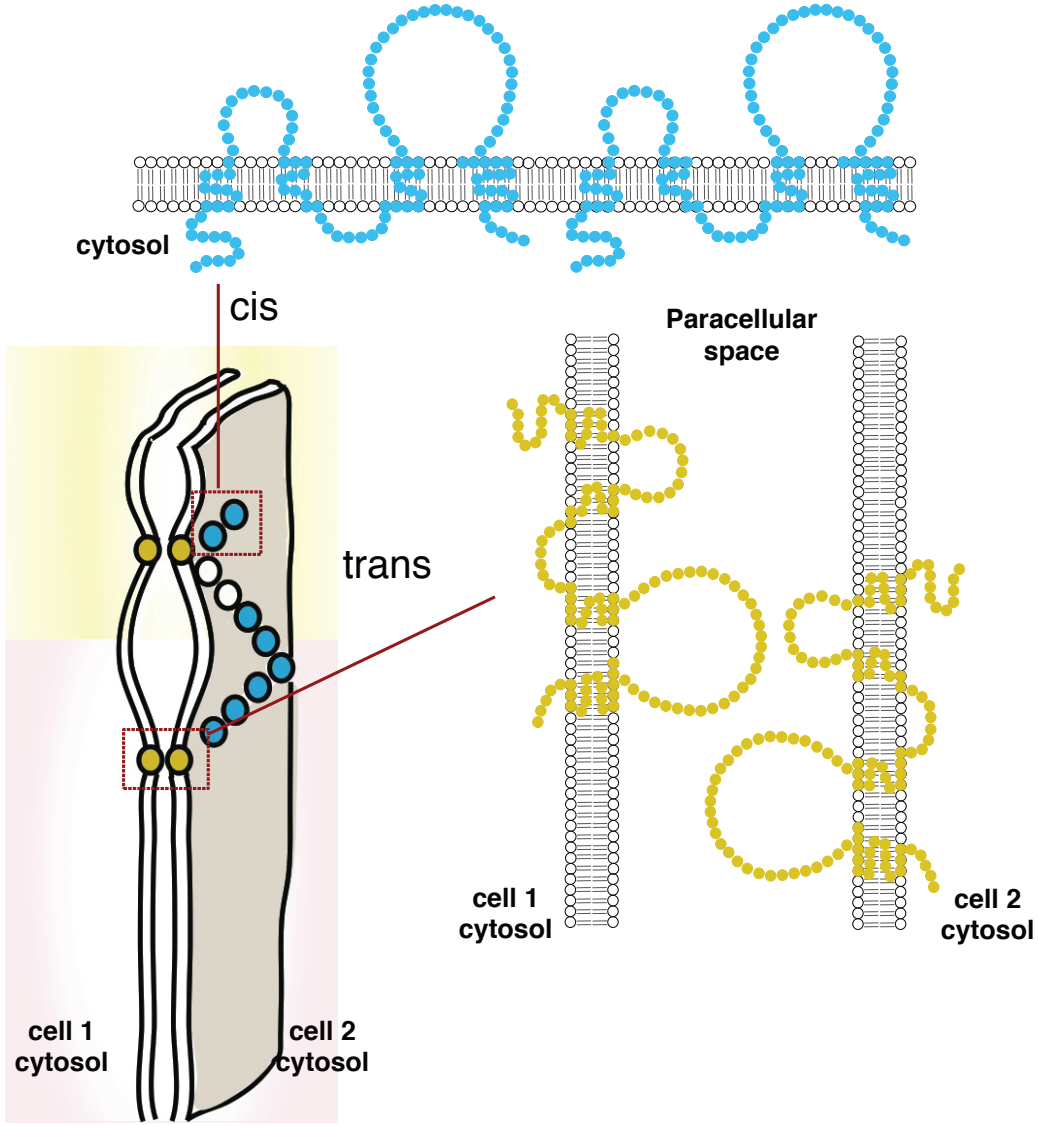

Figure 1.2 *Claudin interactions.* Diagrammatic representation of *cis* (between claudins within the same membrane) and *trans* claudin-claudin interactions (head-to-head, between claudins in adjacent cells).

was used to describe the existence of domains within the first and second extracellular loops important for mediating the *trans* or head-to-head interactions across the paracellular space (28). Although various compatible claudins have been identified, so far there is very little information about the significance of their binding. The best-studied case in the literature is the interaction between claudin -16 and -19, which is essential for their incorporation into the tight junction and the formation of a cation selective tight junction complex in the thick ascending limb (45, 46). Similar results were observed in a recent study using cortical collecting duct cells, which reports that interaction between claudin-4 and claudin-8 is necessary for claudin-4 assembly at the tight junction (47). The claudin composition and interactions at the epithelial tight junction are the sole determinants of paracellular properties of that epithelium. As more information about claudins emerges in the literature, it may become possible to predict tight junction electrophysiology based only on claudin expression.

1.4.6 Claudins in the proximal tubule

A complete investigation of claudin expression in the proximal tubule has yet to be performed. However, the presence of some claudin isoforms has been confirmed, including claudins -2, -10, -11 (55) and -4 (83). Claims of claudin -11 expression were later retracted due to probable cross-reactivity of the claudin-11 antibody with claudin-10 (77). The presence of claudin -6 and -9 was observed in the proximal tubule of neonatal, but not adult mice (1). Altogether, the information about the function of claudins in the proximal tubule is relatively vague, with the exception of claudin-2, which forms a cation selective pore

(37,77). Model systems such as MDCK and LLC-PK1 cells have been commonly used to study claudins, but each cell line comes with certain limitations.

1.5 Common model systems for studying Claudins in the proximal tubule

1.5.1 MDCK cells

According to Dukes *et al.* there are at least six strains of MDCK cells (30). A heterogeneous population of epithelial cells was originally isolated in 1958 from the kidney of an adult female cocker spaniel. This is the parental MDCK (NBL-2) line (66) from which MDCK I and MDCK II cells were derived. The difference between the two strains lies mainly in their resistance characteristics (12, 84). While MDCK I cells are very tight (TER ~4000 Ω cm^2), MDCK II cells rarely reach over 100 Ω cm^2 (12). The resistance discrepancies are also accompanied by ion selectivity differences. Namely, MDCK II cells are highly cation selective (pNa^+/pCl^-=10 (7)), while MDCK I cells are much less so (pNa^+/pCl^- =1.7 (73)). This variability is most likely due to differences in claudin expression. Although claudin -1, -3, -4, and -7 expression was demonstrated in both strains, claudin-2 can be found only in MDCK II cells (37, 95). This is consistent with the previously described function of claudin-2 as a cation selective channel. According to some investigators, MDCK II cells resemble the proximal tubule, while MDCK I cells correlate with more distal portions of the nephron (11, 84, 90, 97). However, compared to the proximal tubule *in vivo*, MDCK II cells have much higher resistance and cation selectivity. 'Anion selective' claudins are often introduced into the highly cation selective background of MDCK II cells, to find a decrease in cation permeability. Namely, claudin- 4, -5, -8, -11 and -14

significantly decreased cation permeability in these cells (15, 25, 102, 108, 111). One cannot safely conclude that the expression of these claudins would have the same effects in the proximal tubule, an epithelium, which is already much less cation selective. Regardless of all the differences, MDCK II cells are often used to draw conclusions about the proximal tubule epithelium (61, 70, 86, 89, 90). Even more surprising is the use of the anion selective porcine kidney cell line – LLC-PK1 cells (48), as a representative of the proximal tubule.

1.5.2 LLC-PK1 cells

The LLC-PK1 epithelium is strictly anion selective ($pNa^+/pCl^- = 0.42$) and highly resistant when compared to the proximal tubule *in vivo* (TER= 127 Ω cm^2)(82). Expression of claudins -1, -3, -4, and -7 has been demonstrated in this cell line (43). More claudins may be identified in LLC-PK1 cells, pending a comprehensive investigation of all isoforms. Expressing anion selective claudins in this type of cell line may not have an electrophysiological effect. Instead, most exaggerated results are obtained by the expression of cation selective claudins. To this end, claudin -2, -15 and -16 were found to selectively increase cation permeability in LLC-PK1 cells (44, 104). Unfortunately, due to a huge difference in baseline characteristics such as TER and ion selectivity, these results may not apply to the proximal tubule.

1.5.3 Importance of the model system baseline characteristics

It is not uncommon for a claudin isoform to have dramatic effects when expressed in one cell line, but no effect whatsoever when expressed in another. A study by Van Itallie and colleagues (104) demonstrated that the expression of cation selective claudins -2 and -15 has no detectable effects on the already cation selective MDCK II cells, but increases cation selectivity in the anion selective LLC-PK-1 cells. Similarly, anion selective claudins -4 and -11 had no effect on LLC-PK1 cells, but decreased cation selectivity in MDCK II cells. The same phenomenon was later described for claudins -7 and -16, both of which increase cation selectivity in LLC-PK1 cells, and lack a detectable effect on MDCK II cells (3, 44). Therefore, the effect of claudin expression is intimately linked with the endogenous properties of the cell line used. These specific properties likely preclude claudin effects on ion selectivity and resistance alike. For example, expression of claudin-15 in MDCK II cells results in increased TER (25), but in LLC-PK1 cells, its expression decreases resistance (104). The same discrepancy was demonstrated for claudins -11 (104), and -16 (44, 49). These results are further complicated by claudin knockdown studies in LLC-PK1 cells and MDCK II cells (43). Both model systems express claudin-4 and its knockdown in MDCK II cells increases cation permeability. In LLC-PK1 cells the knockdown of claudin-4 leads to decreased chloride flux and altogether a loss of anion selectivity. This is consistent with the role of claudin-4 as an anion selective claudin. In the same study, a TER decrease in MDCK II and increase in LLC-PK1 cells was observed as a direct result of claudin-4 knockdown. This data is

seemingly contradictory. However, one can argue that it is consistent if somehow claudin-4 forms a cation barrier in MDCK II cells and an anion channel in LLC-PK I cells, by interacting with endogenous claudins. Alternatively, it is also possible that the electrophysiological effects are due to a secondary alteration in the expression of other claudins. Nonetheless, this data is inconsistent with results of another experiment where Van Itallie *et. al.* found an increase in LLC-PK1 resistance upon claudin-4 expression (104). The model systems available to study the function of claudin-4 represent two extreme epithelial environments, one strongly cation selective and another strongly anion selective. The results of claudin-4 expression in these cell lines are interesting but not representative of the proximal tubular epithelium, where the expression of claudin-4 has been demonstrated (83). Moreover, the expression of endogenous claudin isoforms has not been exhaustively characterized in either model system, making the assessment of perturbations in other claudin expression difficult.

It would therefore be beneficial to explore and characterize new model systems for studying claudin function in a lower resistance, less ion-selective environment. Existing model systems of very loose epithelia include OK cells (opossum), NRK-52E (rat), HK2 (human), and HRPTE (human) cells. The latter two cell systems are not suitable for studying paracellular fluxes because even after 2 weeks in culture, HK2 and HRPTE cells fail to form tight junctions (81). Of the remaining two, preference was given to OK cells. This is because OK cells endogenously express the PT protein NHE-3, and are therefore, more commonly used to represent the proximal tubule (2, 5, 6).

1.6 OK cells

Opossum Kidney cells were isolated from the kidney of an American opossum, species *Didelphys virginiana* (57). The opossum genome has been sequenced and published, however it is from the small grey tailed opossum, *Monodelphis domestica*. Therefore, one expects small variations in gene sequence in OK cells due to genetic drift (71). An in-depth analysis of paracellular permeability, performed using OK and LLC-PK1 cells, concluded that OK cells are better suited for studying the proximal tubule (63). Like the proximal tubule, OK cells have a very low transepithelial resistance of < 40 Ω cm^2 (81, 92). The apparent paracellular permeability coefficient of OK cells (P_{app} = 12.17 ×10^{-6} cm/sec) was also reported to be remarkably similar to that of the proximal tubule (63). However, OK cells have not been explored in terms of ion selectivity and their tight junction molecular composition.

1.7 Hypothesis

We propose that OK cells will have electrophysiological permselectivity properties and a claudin expression profile similar to the proximal tubule. The over-expression of claudin-4 and claudin-2 in OK cells will help clarify their function.

1.8 Objectives:

1. Determine the electrophysiological and molecular characteristics governing paracellular transport across the loose epithelial cell culture model, OK cells.
2. Use OK cells to study the function of claudin-4 and claudin-2.

Chapter 2:

MATERIALS AND METHODS

2.1 Cell culture and stable cell lines

All cell lines were originally obtained from ATCC (Rockville, MD, USA). OK and LLC-PK_1 cells were maintained in DMEM/F12 medium, supplemented with 10% fetal bovine serum (FBS) and 5% penicillin streptomycin glutamine (PSG) at 37°C in a 5% CO_2 incubator. HEK 293 and MDCKII cells were maintained in DMEM, containing 10% FBS and 5% PSG.

Polyclonal stable cell lines expressing claudin-4HA, mouse claudin-2HA and pcDNA3.1$^+$ (Invitrogen) were created by transfecting plasmid DNA into OK cells with Fugene 6, then selecting for transfected cells with 750 μM G418 (Invitrogen). To make monoclonal stable cell lines, the polyclonal stable cells were plated with limiting dilutions so that individual colonies could be selected and grown to confluence in the presence of 750 μM G418. Expression of claudin-2 and claudin-4 in individual stable cell lines was confirmed by immunofluorescence microscopy, immunoblot and quantitative RT-PCR.

2.2 Antibodies

The following primary antibodies were employed: rabbit polyclonal anti-claudin-4 (Thermo Scientific, Waltham, MA, USA), mouse anti-HA (16B12, Covance, Mississauga, ON, Canada) and rabbit anti-ZO-1 (Invitrogen, Carlsbad, CA, USA). Secondary antibodies used were: horseradish peroxidase conjugated donkey anti-rabbit and goat anti-mouse (Santa Cruz Biotechnology Inc., Santa Cruz, CA, USA) as well as DyLight 488 Conjugated AffiniPure donkey anti-rabbit and DyLight 549 conjugated AffiniPure donkey anti-mouse (Jackson ImmunoResearch Laboratories, West Grove, PA, USA).

2.3 Molecular Biology

2.3.1 Expression PCR

To examine claudin expression in OK cell cDNA, two sets of degenerate PCR primers for each claudin gene were designed based on the NCBI sequence of the *Monodelphis domestica* opossum (71) (Table 2.1). This approach was necessary as OK cells were derived from *Didelphis virginiana* (57) and therefore contain intrinsic genetic differences. Three different templates were utilized for PCR: genomic DNA (extracted directly from OK cells), cDNA (generated by reverse transcription of OK cell RNA isolated 5 days after plating) and no reverse transcriptase cDNA (generated as per cDNA, but without the addition of reverse transcriptase). A 1.5% agarose gel was used to analyze which claudins are expressed based on the amplification of the appropriate size product from cDNA. The presence of each claudin detected was confirmed by cloning it from this cDNA.

2.3.2 Cloning and plasmid construction

pcDNA 3.1^+ (Invitrogen) and pGEM® -T Easy (Promega, Madison WI, USA) vectors were utilized to generate constructs containing the claudin genes we found to be expressed in OK cell cDNA. We also cloned glyceraldehyde 3- phosphate dehydrogenase (GAPDH). All sequences were cloned by PCR, using homologous primers to the *Monodelphis domestica* or *Mus Musculus* (claudin-2) sequence found in the NCBI database. For claudins -2, -4, -9 (variant 1), -11, -12, and GAPDH, the PCR product was shuttled directly into pcDNA 3.1^+. For these constructs, a Kozak (58) sequence was introduced between the restriction site and

	Forward (set 1)	Reverse (set 1)	Forward (set 2)	Reverse (set 2)
Cldn 1	AGTTGCTGG GCTTCATCCT	GTCGAAGAC TTTGCACTGG A	CAGTTGCTGG GCTTCATCCT G	GAGTCGAAGA CTTTGCACTG GATC
Cldn 2	TGGCTTCTA GTGCCATCT CC	TCGAACTTCA TGCTGTCAGG	GGTGGCTTCT AGTGCCATCT C	CTCGAACTTC ATGCTGTCAG GC
Cldn 3	AAGGTGTAC GACTCGCTG CT	ACGTAGTCCT TGCGGTCGTA	CAAGGTGTAC GACTCGCTGC	CGTAGTCCTT GCGGTCGTAG
Cldn 4	AAGGTGTAC GACTCGCTG CT	GGGTTGTAG AAGTCCCGG AT	-	-
Cldn 5	CCTGGAAAG CAACATTGT GA	CCACAGAGC ACATAGAGC GA	CGGCCTTCCT GGAAAGCAA C	GCCACAGAGC ACATAGAGCG AG
Cldn 6	CCTGTATGCT GGACTGCTC A	TACTCAGAA GGACCTCGG GA	CCCTGTATGC TGGACTGCTC	GTACTCAGAA GGACCTCGGG AG
Cldn 7	CAACTGTTG GGGTTCACC AT	CAGGCAGAG CCAAGACTG A	ACTGTTGGGG TTCACCATGG	AGGCAGAGCC AAGACTGAG
Cldn 8	TCAGGATGC AGTGCAAAA TC	TTCTCGTTTC TGAGCCGAA T	CGCCAACATC AGGATGCAGT	GGGCTTCTCC TAGTTCTCGT
Cldn 9	TCTGCTGGT GGCTATCAC TG	AGGTGCAGC ATAGCAGTC CT	GTCTGCTGGT GGCTATCACT GG	GGTGCAGCAT AGCAGTCCTC
Cldn10	ATCATCGCC TTCATGGTA GC	ATGTAACCGT CCAGAGCCA G	GATCATCGCC TTCATGGTAG CT	CAGCATGGAG GGGAAGTCCT
Cldn11	GCAACTGGT TGGATTTGT GA	GAGGATGTC CACGAGTGG T	CTGCAACTGG TTGGATTTGT GACG	AGGATGTCCA CGAGTGGTTT G
Cldn12	CGGGATGTC CATGCAGCA AC	CTGGTCCACC GAGGAATAC C	-	-
Cldn14	CTCCTGGGTT TCTTGCTCAG	ATTGGTGGTC CAGGAGACA G	CCTGGGTTTC TTGCTCAGCT	TTGGTGGTCC AGGAGACAGC
Cldn15	GCTGGGGCT ACTAATGCT TG	GCAAGCATG GAAGGAAAC TC	CGCTGGGGCT ACTAATGCTT GG	GGCAAGCATG GAAGGAAACT CC
Cldn16	CAGGTGTTC CTGGGATTG TT	CAGCAAGTG AGGACTGCT CC	TCCTGGGATT GTTGGCTCTG	GCAAGTGAGG ACTGCTCCAG

	Forward (set 1)	Reverse (set 1)	Forward (set 2)	Reverse (set 2)
Cldn17	CCTTCATTGGGAGCAACATT	CCCTGATGATGAGATTGGCT	GTCTGCCTTCATTGGGAGCA	ATTGGCTGTCCAGGACACAG
Cldn18	ACTCTTTGCCAAATGATGGG	AGCTGGAAGACCAAGAATAGTG	CGACTCTTTGCCAAATGATGGGG	ATGGTCGGCACTCAGTTAACCC
Cldn19	AACTCTGGCTTCCAGCTCCT	GACATCCAGAGCCCTTCGTA	CAACTCTGGCTTCCAGCTCC	GGACATCCAGAGCCCTTCGTAG
Cldn20	GGTAAATGCAAATGTGGGCT	CCTGGCTTCTTGATGCATTT	AAGGGCTGTGGATGGATT**G**C	GGAGGGTAGAACCTGGCTTC
Cldn22	ACTCTGGCAGACTTGCGTTT	AACCCAGGACACTGGAATGA	GGACTCTGGCAGACTTGCGT	CCCAGGACACTGGAATGAGG
Cldn23	GCTGGGCTACTATGAGGCTG	TTTTGCAGGACATGGGTGTA	GAGCTGGGCTACTATGAGGC	GCGGTTTTGCAGGACATGGG

Table 2.1 *Opossum Kidney Claudin PCR primers*. Two sets of primers were used for each claudin isoform, generated from the NCBI sequence of *Monodelphis domestica*. A dashed line instead of the second set of primers indicates that only one set of primers was necessary to identify expression of that particular claudin.

	Forward primer	Reverse primer
Claudin-1	5'-ATG GCC AAC GCG TTG-3'	5'-TCA CAC ATA GTC CTT TCC ACT GGA GG-3'
Claudin-2	5'- CGC GGA TCC GCC ACC ATG GCC TCC CTT GGC GTT-3' (BamHI site)	5'-CCG GAA TTC TCA CGC ATA GTC AGG AAC ATC GTA TGG GTA CAC ATA CCC AGT CAG GCT G-3' (EcoRI site)
Claudin-4	5' -CGC GGA TCC GCC ACC ATG GGG TCC ATG GGG CTCC-3' (BamHI site)	5' -CCG GAA TTC TCA CGC ATA GTC AGG AAC ATC GTA TGG GTA CAC GTA GTT GCT GGT AGG GGC -3' (EcoRI site)
Claudin-6	5'- ATG GCT TCT GCC GGC CTC C -3'	5'- TTA TAC ATA ATT CTT GGC CTG GTA CTC AG -3'
Claudin-9	5' -CGG GGT ACC GCC ACC ATG GCT TCA GCT GGG CTG G -3' (KpnI site)	5' - GGA ATT CTC ACG CAT AGT CAG GAA CAT CGT ATG GGT ACA CAT AAT CCC GTT TGT CCA GG -3' (EcoRI site)
Claudin-11	5' -CGC GGA TCC ATG GTT GCC ACT TGC CTG C -3' (BamHI site)	5' -CCG GAA TTC TCA CGC ATA GTC AGG AAC ATC GTA TGG GTA TAC GTG GGC ACT CTT GGC G -3' (EcoRI site)
Claudin-12	5' -CGC GGA TCC GCC ACC ATG GGT TGT CGG GAT GTC CAT GC -3' (BamHI site)	5' -CCG GAA TTC TCA CGC ATA GTC AGG AAC ATC GTA TGG GTA GGT GGC GTG GCT CAC CAC AGG -3' (EcoRI site)
Claudin-15	5'- ATG TCA GTT GCT GTA GAG ACA TTT GGA- 3'	5'- CTA TAC ATA GGC ATT TTT CCC ATA TTT GCC -3'
Claudin-20	5'- ATG GCA TCA TCA GGT CTA CAG CTC C- 3'	5'- TCA TAC ATA ATC CTT CAG GTT GTA GCC TGC- 3'
GAPDH	5' -CCC AAG CTT ATG TCC AAG GTG CAC ATT AGT AGA TTT GG -3' (HindIII site)	5' -CCG GAA TTC TCA CGC ATA GTC AGG AAC ATC GTA TGG GTA CTC CTT GGT GGC CAT GTA CG -3' (EcoRI site)

Table 2.2 *Primers and restriction sites used for cloning the Opossum Kidney Claudins and mouse claudin-2.* Primers used for amplification and cloning of each claudin expressed in the *Didelphis virginiana* opossum cDNA library, and claudin-2 from mouse kidney cDNA.

the coding sequence in the 5' primer (except for claudin-11 and GAPDH) and an HA tag was inserted before the stop sequence in the 3' primer. The genes were amplified by PCR from the OK cell cDNA library or mouse kidney cDNA (for mouse claudin-2) using primers with unique restriction enzyme sites (Table 2.2). PCR products were then digested with enzymes corresponding to the unique restriction sites, and ligated into the pcDNA 3.1^+ vector that was previously linearized using the same restriction enzymes. The gene in each construct was sequenced and compared to the *Monodelphis domestica* sequence using the Emboss Pairwise Alignment tool (http://www.ebi.ac.uk/Tools/psa/emboss_needle/nucleotide.html). For the cloning of claudin -1, -6, -15 and -20, primers without an HA tag or restriction sites were designed corresponding to the extreme 5' and 3' coding sequence (Table 2.2). PCR was performed using these primers and products were inserted into pGEM®-T Easy by ligation. Each gene was sequenced and compared to the corresponding sequence from the *Monodelphis domestica* opossum. We were only able to clone a truncated version of claudin-15 from the *Didelphis virginiana* opossum cDNA generated (data not shown). All sequences obtained were deposited into the GenBank Database.

2.3.3 Quantitative Real-time PCR

RNA was isolated from OK cells (seeded at 3 x 10^6/10 cm dish and harvested at day 5) using a Qiagen RNA isolation kit. For qRT-PCR experiments on cells after siRNA knockdown, RNA was isolated by the same means, however cells were seeded at 6 X 10^5 and they were collected 96 hours after transfection. Random primers, SuperScript II reverse transcriptase (Invitrogen) and 1 μg of RNA, were

used to generate cDNA that was then employed to quantify the expression of each claudin gene and the GAPDH gene. This experiment was performed in triplicate.

IDT software (Integrated DNA Technologies Inc., San Diego, CA, USA) was used to design Taqman quantitative real-time PCR primers and probes, based on the cloned sequences of the *Didelphis virginiana* opossum claudins (Table 2.3). To determine the absolute claudin expression, plasmid standards of each of the previously described claudin constructs were diluted into concentrations ranging from 0.000002 pg/µl to 2 pg/µl, and used to generate standard curves corresponding to each gene. A linear relationship was established between copies of claudin and fluorescence intensity, which was then used to calculate the copies of each claudin in the experimental OK cDNA samples. For the purposes of comparing the expression levels of claudins between different stable cell lines, standards were generated by dilution of control cDNA and the quantity of claudin expression was normalized to GAPDH for each cDNA sample. Expression levels were quantified using an ABI Prism 7900 HT Sequence Detection System (Applied Biosystems Inc., Foster City, CA, USA).

Claudin-1	**F** - GAATTCTATGATCCCCTGACCC **Probe** – /56- FAM/CTCCTTTGCTGTTCCTGTCCCAAGA/3IABLFQ/ **R**- AGGAGTCGGGTAAGAGGTTG
Claudin-4	**F**- CTCCAGGTAGTGGGCATTG **Probe**- /56- FAM/CCTTCATCGGCAGCAACATCGTG/3IABLFQ/ **R**- ACACAGTTCATCCACAGGC
Claudin-6	**F**- CGTCTTGTACTGACTTCTGGG **Probe**- /56- FAM/TGCTGGACTGCTCATGCGATCA/3IABkFQ/ **R**- CAACTCCCGTTTCTGGACTC
Claudin-9	**F-** GTGTGGAAGATGAGGTGGC **Probe-** /56- FAM/AGGACCAGGATCCCAGAGATGAGG/3IABkFQ/ **R-** CACCAGAGGATTGTAGAAGTCC
Claudin-11	**F**- AGATTGTGTCATGGCTACGAG **Probe**- /56- FAM/AGGTTATGTCCAGGCTTGCCGAG/3IABkFQ/ **R**- ACAGTCAAGAGCAGGAAGATG
Claudin-12	**F**- TGCTGTTCTTGTGGTACTGTG **Probe** - /56- FAM/TCTGGCCGAGTAGGGCTGAGAATA/3IABLFQ/ **R**- ACAGGGATGTCTATCTCGATGG
Claudin-15	**F**- CCACCTCGACCATCTTTGAG **Probe** - /56FAM/TCCTTCCATGCTTGCCCTGTCTG /3IABLFQ/ **R**- ATAGCTGTGATCATGAGTGCC
Claudin-20	**F**- GGTAAATGCAAATGTGGGCTC **Probe**- /56FAM/ATGGTACAGCACCGGGATGTTC AG/3IABkFQ/ **R-** CACATACACAGGAAGGGCTAG

Table 2.3 *Opossum Kidney Claudin qRT-PCR primers and probes.* Successful probes and primers used in the quantitative real-time PCR experiments with claudins -1, -4, -6, -9, -11, -12, -15, and -20 in OK cells.

2.3.4 siRNA knockdown

Claudin-4 knockdown was performed in monoclonal stable cell lines expressing claudin-4HA and pcDNA 3.1^{+}. Two different siRNA sequences against the opossum claudin-4 sequence cloned were designed using Thermo Scientific Dharmacon RNAi Technologies siDESIGN center software and then synthesized (Dharmacon Inc., Lafayette, Colorado USA). The sequences were: #1 5'-AUG GUC UUG GCC UUG GAG GUU-3' and #2 5'-UCA UCC ACA GGC CCU AUU-3'. As a control, each sequence was scrambled using GenScript software (GenScript USA Inc., Piscataway, NJ USA): scrambled #1 5'-AGG CUC AUG CGG UUG UGG UUU-3' and scrambled #2 5'-GCU CUA ACA CCC UCC AGC CUU-3'. The cells were seeded at 6 X 10^5 cells/snapwell insert for Ussing chamber experiments or into each well of a 6-well plate for qRT-PCR, and transfected with 200nM scrambled siRNA or claudin-4 siRNA using Oligofectamine (Invitrogen) according to the manufacturer's protocol. 96 hours post-transfection, the cells were collected for qRT-PCR or mounted in Ussing Chambers for dilution potential studies.

2.4 Expression and Localization studies

2.4.1 Immunoblot analysis

HEK 293 cells (plated at 3 X 10^6 cells/10 cm dish) were transfected with pcDNA 3.1^+ or claudin-4HA and then harvested after 48 h using the protocol described below. Cells were resuspended in 400 µl of SDS-PAGE sample buffer containing 4.6% SDS, 0.02% Bromphenol Blue, 20% Glycerol, 2% 2-ME, 130mM Tris-HCl, pH 6.8 and a protease inhibitor cocktail (Calbiochem, Gibbstown, NJ, USA), then mechanically sheared by passing through a 23-gauge needle. The lysates were subjected to SDS-PAGE under denaturing conditions and then transferred to a nitrocellulose membrane. Prior to incubation with the antibodies, the membrane was blocked overnight with 5% milk in Tris-Buffered Saline and 0.1% Tween 20 (TBST). Primary antibodies (1:1000) were applied at 4°C overnight, followed by a two-hour incubation with horseradish peroxidase coupled secondary antibodies (1:5000) at room temperature. Proteins were detected with Western Lightning™ Plus ECL reagents (PerkinElmer Inc., Boston, MA, USA) and visualized using a Kodak Image Station 440CF (Kodak, Rochester, NY, USA).

2.4.2 Immunohistochemistry

For transient transfections, OK cells were seeded on glass coverslips, transfected with pcDNA 3.1^+ or claudin-4HA using Fugene 6, and then fixed using 4% paraformaldehyde (PFA) 24 h later. The stable cell lines were plated and allowed to reach confluence before immunofluorescence studies (>5 days). Prior to incubation with antibodies, the cells were washed three times with Phosphate-Buffered Saline (PBS) containing 1 mM $CaCl_2$ and 1 mM $MgCl_2$, fixed with 4%

PFA, and quenched with 5% glycine in PBS, then permeabilized with 0.2% Triton-X100 and blocked with 5% milk in PBS. Antibodies and 4',6-diamidino-2-phenylindole (DAPI) were applied at a dilution of 1:500 in 5% milk in PBS, for 1 h at room temperature. Finally, the samples were mounted with Dako (Dako, Glostrup, Denmark) and analyzed using a custom assembled spinning disc confocal microscope detailed in (52).

2.5 Functional studies

2.5.1 Ussing Chamber Experiments

Opossum kidney cells and stable cell lines were seeded at 1 X 10^5 cells on 6 well Snapwell inserts (Corning, NY, USA) and grown to confluence (day 5). For claudin-4 knockdown experiments, cells were seeded at 6 X 10^5 and mounted 96 hours after transfection. Ussing Chamber studies were carried out with slight modifications to published procedure (44). Initially, we corrected for baseline conditions of empty Ussing Chambers with Buffer A (145 mM NaCl, 1 mM $CaCl_2$, 1 mM $MgCl_2$, 10 mM glucose and 10 mM HEPES, pH 7.4) at 37 °C. The Snapwell inserts with confluent OK monolayers were washed three times using Buffer A and then mounted between the two hemi-chambers, both of which were filled with 10 ml of Buffer A (Figure 2.1). Current clamps were performed using a DVC 1000 I/V Clamp (World Precision Instruments, Sarasota, FL, USA) and electrodes containing an agarose bridge with 3 M KCl. Data were acquired as a trace and recorded using PowerLab (ADInstruments, Colorado Springs, CO, USA) running Chart 4.0 software. To determine the TER and permeability properties of the epithelia, a 90 μA current was applied across each monolayer

and a dilution potential was induced by replacing Buffer A in the apical hemi-chamber with Buffer B (80 mM NaCl, 130 mM mannitol, 1 mM $CaCl_2$, 1 mM $MgCl_2$, 10 mM glucose, and 10 mM HEPES, pH 7.4). The osmolality of the buffers, measured using an Advanced Osmometer, model 3D3 (Advanced Instruments, Norwood, MA) was 310 ± 10 mmol/kg water. TER measured was quite small (11 ± 1 Ω cm^2) and the variation in the intrinsic resistance of Snapwell filters was considerable, relative to the low resistance of the confluent monolayer. To eliminate this variability, the dilution potential and resistance of each filter were determined following removal of the cells by trypsinization (30 min at 37 °C) and this measurement was subtracted from the values generated by that specific filter with cells grown on it. The Goldman-Hodgkin Katz and Koketsu (53) equations were used as described previously (44) to calculate the absolute permeability of sodium and chloride, and to determine the relative permeability of sodium to chloride (pNa^+/pCl^-). The permeability of Br^-, I^-, K^+, Li^+, Cs^+ and Rb^+ were obtained by the same protocol, except NaCl was substituted for an equimolar concentration of NaI, NaBr, KCl, LiCl, CsCl and RbCl in both buffers A and B. Osmolality of these buffers were similar to the Na containing buffers.

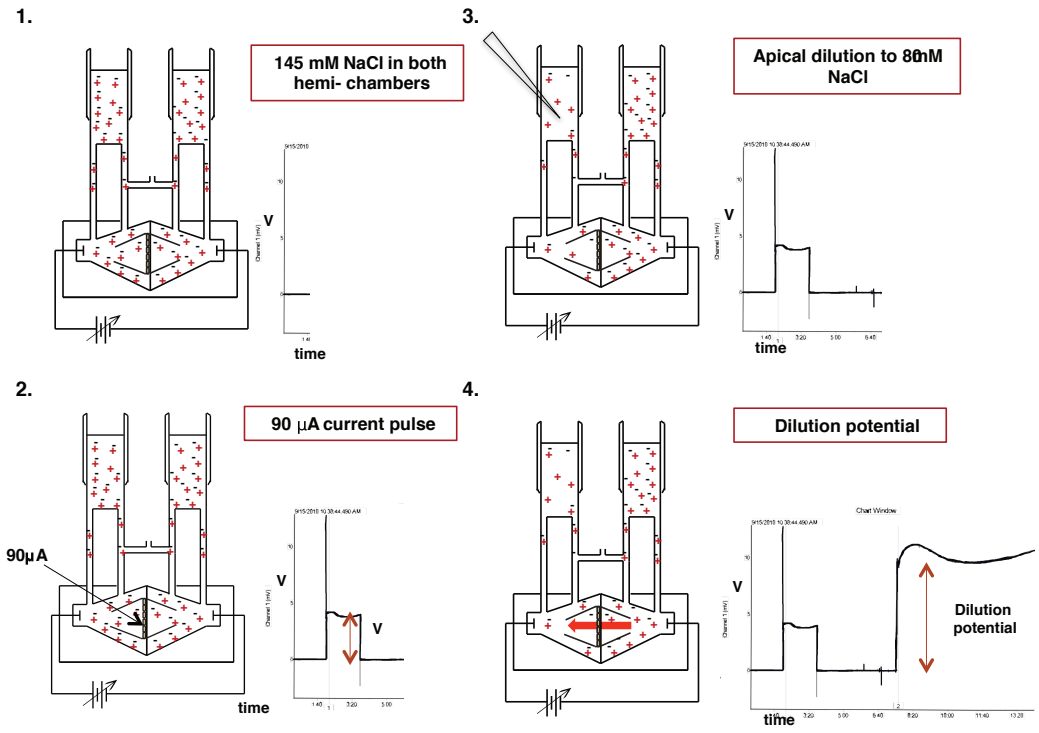

Figure 2.1 *Representative Ussing Chamber Dilution Potential measurment*. Diagrammatic representation of the Ussing Chamber Apparatus and accompanying Chart recording of voltage *vs* time. Following a 30 minute equilibration period (Step 1), a 90 µA pulse is applied to the cell epithelium (situated between the two hemi-chambers, apical facing left) to produce a voltage peak (Step 2) and Buffer A in the apical compartment is replaced with Buffer B inducing a dilution potential (Step 3 and 4).

2.5.2 Fluorescent Dextran Flux

The Fluorescent Dextran molecules used for paracellular permeability studies were Alexa Fluor 488 (MW- 3 kDa, anionic), Texas Red (MW- 3 kDa, neutral) and Rhodamine B (MW- 70 kDa, neutral) from Invitrogen. OK cells expressing empty vector or claudin 4 were seeded on 24 well Snapwell inserts (Corning, NY, USA) at a concentration of 4 X 10^4 and allowed to reach confluence (Day 5). On the day of the experiment, both apical and basolateral compartments were washed using Fluorescence Buffer (10 mM HEPES, 135 mM NaCl, 1 mM $MgCl_2$, 1 mM $CaCl_2$, 3 mM KCl, 10 mM glucose, pH 7.4). While shaking, the cells were incubated with solution containing 40 ng/ml of the Fluorescent Dextran (in the apical compartment) then, in triplicate, 10 µl samples were collected from the basolateral compartment at 0, 5, 10, 20 and 30 minutes. The sample fluorescence was assessed in a 384-well clear optical reaction plate (Applied Biosystems Inc) using a SynergyMx multi mode microplate reader and Gen5 analysis software (Biotek Instruments, Vermont USA). Final fluorescence values were calculated using standard curves obtained by dilution of the appropriate dextran (range: 0.1-1000 ng/ml).

2.6 Statistical Analysis

Data are reported as mean ± SE. Statistical significance was analyzed with Student's t-test and values <0.05 were considered significant.

Chapter 3

RESULTS

The majority of this data has been published in:

Borovac J, Barker RS, Rievaj J, Rasmussen A, Pan W, Wevrick R, and Alexander RT. Claudin-4 forms a paracellular barrier, revealing the interdependence of claudin expression in the loose epithelial cell culture model, Opossum Kidney Cells. *Am J Physiol Cell Physiol* 2012. Oct 17. [Epub ahead of print]

3.1 OK cells

3.1.1 OK cells form a tight junction

To visualize whether confluent monolayers of OK cells form cell-to-cell contacts, they were immunostained with an anti-ZO-1 antibody, which detects a tight junction associated polypeptide (Figure 3.1A). We observed linear staining at cell-to-cell contacts, suggesting that OK cells do form tight junctions. Confluent monolayers of OK cells were mounted in Ussing Chambers and subjected to increasing current pulses (from -180 μA to +180 μA). Consistent with OK cells having a low resistance tight junction, we observed a slight linear increase in the recorded voltage (Figure 3.1B). Ussing Chambers were also employed to perform dilution potential measurements. Under iso-osmolar conditions induced by adjusting the concentration of NaCl in each hemichamber, we imposed increasing dilution factors across the monolayer and recorded the potential difference (V) generated. We found that the dilution factor imposed correlated linearly with the dilution potential measured across the monolayer (Figure 3.1C).

3.1.2 Tight junction characteristics

To assess the validity of our results and compare them with other model systems, we measured TER and performed dilution potential measurements using MDCK II and LLC-PK_1 cells, along with the OK cells (Figure 3.2). We measured a TER of 41 ± 2 Ω cm^2 for MDCKII cells, 130 ± 5 Ω cm^2 for LLC-PK_1 cells and 11 ± 1 Ω cm^2 for OK cells. A permeability ratio (pNa^+/pCl^-) of 3.2 ± 0.4 was measured for MDCKII cells, 0.9 ± 0.02 for LLC-PK_1 cells and 1.1 ± 0.003 for OK cells. The absolute Na^+ permeability was determined to be 35 ± 1 X 10^{-6} cm/s for MDCKII,

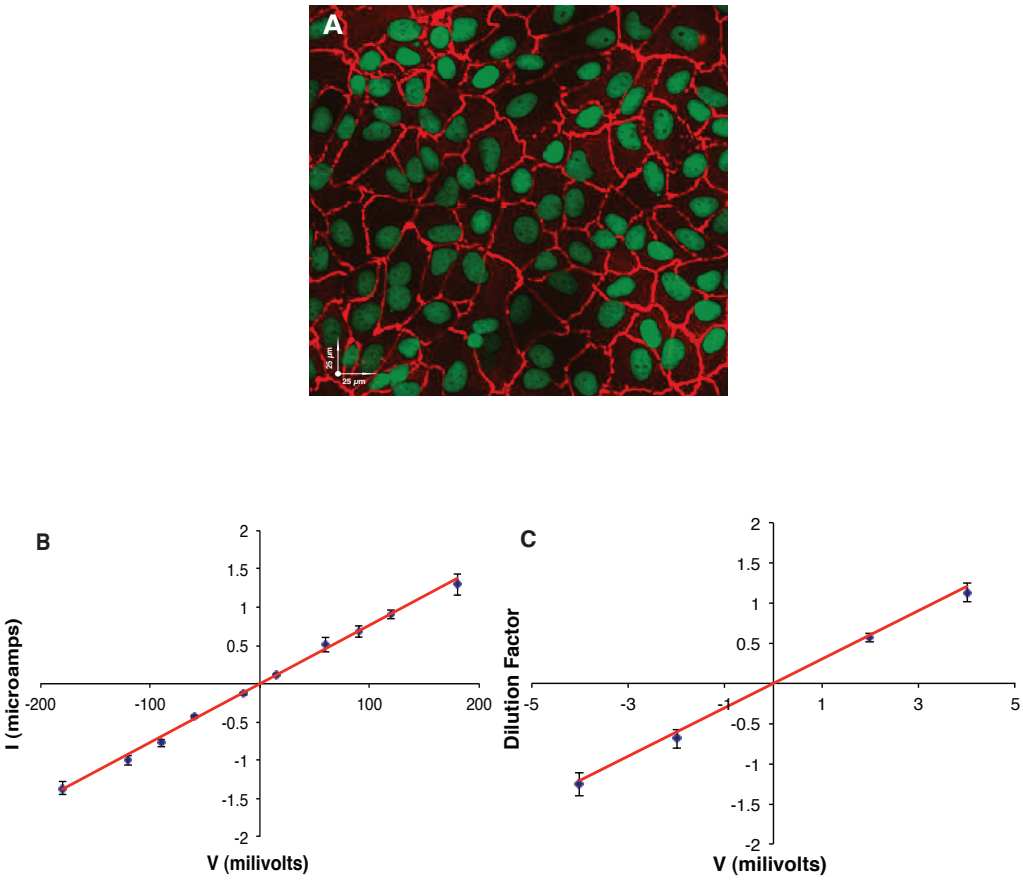

Figure 3.1 *Opossum Kidney cell tight junction* A) Confluent monolayers of Opossum Kidney cells grown on a glass coverslip and immunostained with anti-ZO-1 (red) and Dapi (green). The scale bar represents 25 μm. B) Plot of voltage (mV) measured after the imposition of a current (μA) across OK cell monolayers. C) Plot of potential difference (mV) *vs*. the dilution factor applied across confluent monolayers of OK cells mounted in Ussing Chambers. Data are presented as means ± standard error. Red lines represent a linear fit of the experimental data; the $R^2 = 0.996$ for graph B, $R^2 = 0.995$ for graph C and n =3 for both.

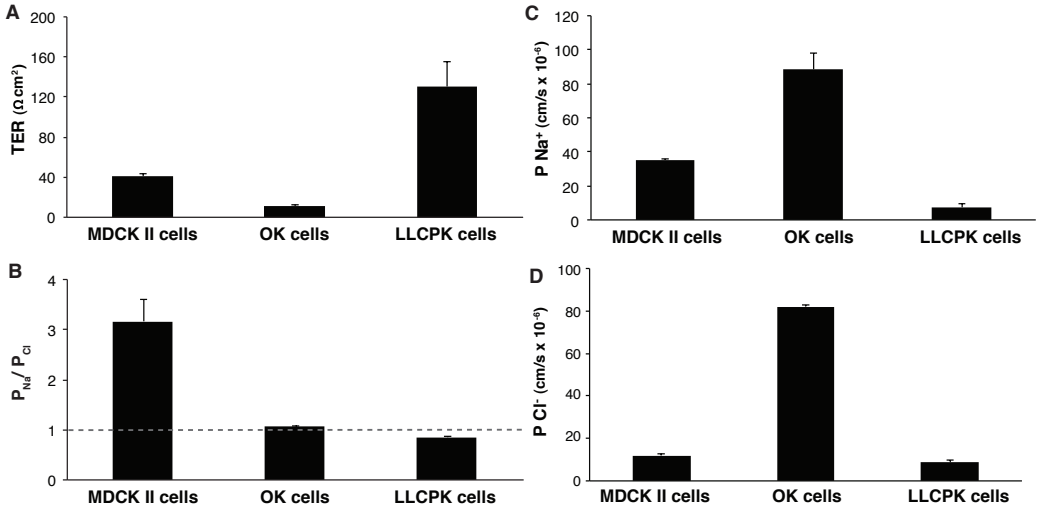

Figure 3.2 *Electrophysiology of MDCKII, OK and LLC-PK1 cells.* Comparison of transepithelial resistance (TER) (A) permeability ratio and (B) absolute permeability of sodium (Na^+) (C) and chloride (Cl^-) (D) across confluent monolayers of MDCKII cells, OK cells and LLC-PK_1 cells, $n \geq 4$ per cell type. Grey dashed line represents a pNa^+/pCl^- ratio of 1. Data are presented as means ± standard error.

7.4 ± 1.8 X 10^{-6} cm/s for LLC-PK_1 and 88 ± 10 X 10^{-6} cm/s for OK cells. Similarly, we measured an absolute Cl^- permeability of 12 ± 2 X 10^{-6} cm/s for MDCKII, 8.6 ± 1.8 X 10^{-6} cm/s for LLC-PK_1 and 82 ± 10 X 10^{-6} cm/s for OK cells (Figure 3.2 D). Thus, compared to the previously described LLC-PK_1 and MDCKII cells, OK cells have a low TER (Figure 3.2 A), are slightly cation selective (Figure 3.2 B) and have relatively high Cl^- and Na^+ permeability (Figure 3.2 C&D).

To further delineate the permeability profile of OK cell tight junctions, we performed dilution potential measurements with other monovalent ions. The permeability sequence of cations (relative to Cl^-) across OK cell monolayers ranks $K^+ >> Cs^+ > Rb^+ > Na^+ > Li^+$. The permeability sequence for anions was $Cl^- > I^- > Br^-$ (Figure 3.3). Next, we turned our attention to identifying the molecular determinants of tight junction selectivity properties in this cell model.

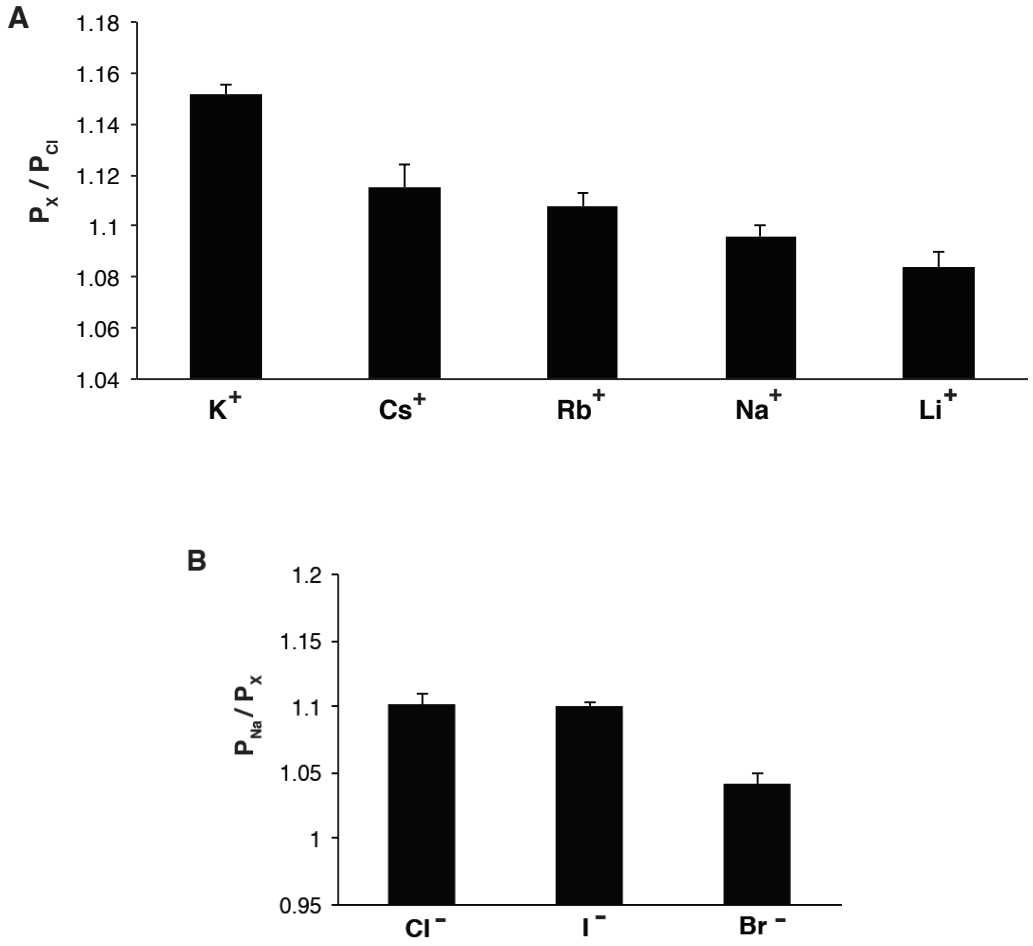

Figure 3.3 *Permeability of monovalent cations across monolayers of OK cells.* OK cell tight junction permeability to cations (K^+, Cs^+, Rb^+, Na^+ and Li^+) with respect to Cl^- and anions (Cl^-, I^-, and Br^-) with respect to Na^+; $n \geq 4$ per ion, data are presented as means ± standard error.

3.2 Claudins in OK cells

3.2.1 Claudins expressed

To determine the endogenous expression of claudins in OK cells, we generated a cDNA library from confluent cell monolayers. We then created two sets of degenerate primers, targeting a single exon for each claudin isoform using the NCBI sequence of the *Monodelphis domestica* opossum (note OK cells were generated from a different species of opossum, *Didelphis virginiana*). Employing these primers, we performed PCR on genomic DNA to test the primer set integrity, cDNA to determine expression of each claudin, and cDNA generated in the absence of reverse transcriptase, to ensure that genomic DNA contamination of the cDNA was not providing a false positive result (Figure 3.4). We included a positive control, GAPDH, and found its expression in both genomic DNA and cDNA, but not in the template lacking reverse transcriptase. In contrast, expression of our negative control, the lens protein crystallin, was found only in genomic DNA, indicating that our cDNA samples were not contaminated with genomic DNA. Using this methodology we observed expression of claudins -1, -4, -6, -9, -11, -12, -15 and -20 in OK cell cDNA (Figure 3.4). It is noteworthy that these results were identical to those observed when cDNA from sub-confluent monolayers of OK cells was used (results not shown).

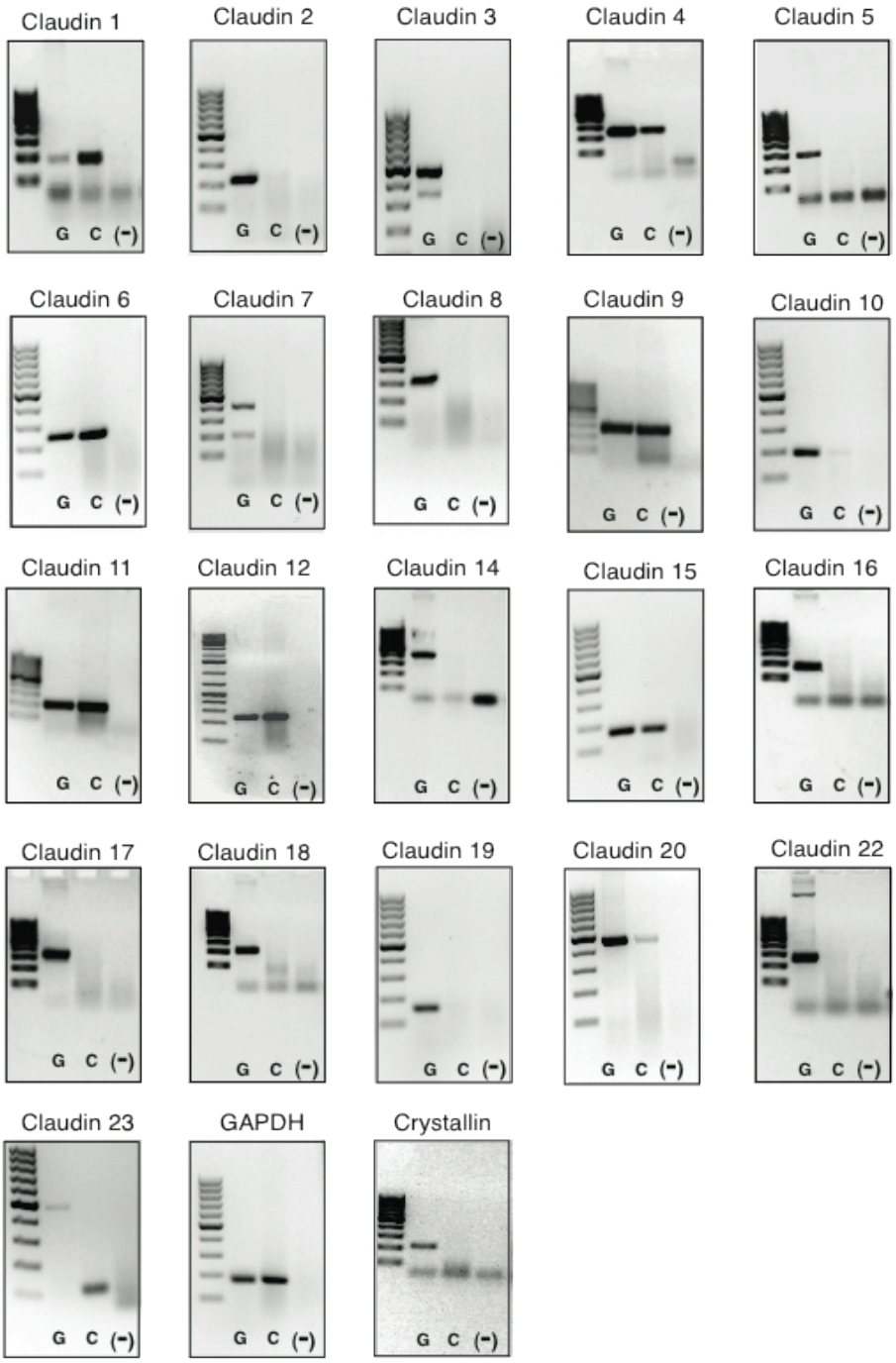

Figure 3.4 *Claudin expression in OK cells.* PCR was performed to identify the expression of each claudin isoform, GAPDH (as positive control) and Crystallin (as a negative control) on three templates: genomic DNA (lane one, abbreviated G), cDNA (lane 2, abbreviated C) and cDNA prepared without reverse transcriptase (lane 3, abbreviated (-)). Final PCR products were electrophoresed on 1.5% agarose DNA gels (with a 100 bp or 1.0 kB ladder), and visualized using ethidium bromide and UV based detection.

3.2.2 Relative claudin expression

In order to quantify the relative expression of each claudin, we cloned the identified isoforms from the OK cell cDNA library and then performed quantitative real-time PCR. Surprisingly, the claudin that was most abundant in this loose, cation selective epithelial cell line was claudin-4, followed by claudin -1 > -6 > -20 > -9 > -12 > -11 > -15 (Figure 3.5). Even though claudin-2 expression in the proximal tubule is well documented (33, 54, 55, 77, 83), we did not find it in our proximal tubule model system. Therefore, in order to study the role of this protein, we introduced mouse claudin-2 into OK cells.

3.3 Claudin-2

3.3.1 Claudin-2 expression and stable cell lines

We generated stable cell lines overexpressing mouse claudin-2 with a carboxy-terminal HA tag (OK/mclaudin-2). Expression of claudin-2 was confirmed by immunoblot analysis (Figure 3.6 A) where a 25kDa band was observed in the stably transfected cells, but not the cells expressing the empty vector. Expression was also confirmed by immunofluorescence (Figure 3.6 B) where co-localization of claudin-2 (HA panel, red) with the tight junction marker ZO-1 (green) was observed. These cells were used for Ussing chamber studies and qRT-PCR.

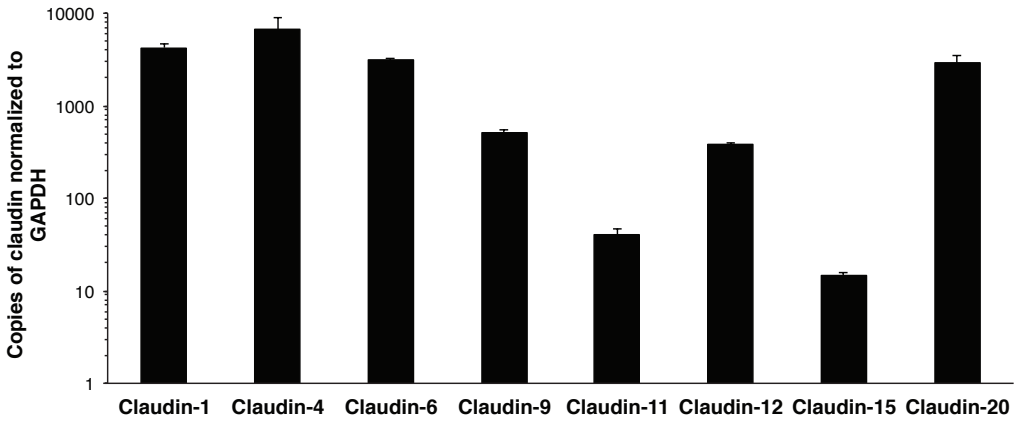

Figure 3.5 *Relative expression of claudins in OK cells.* Quantitative RT-PCR analysis of claudin expression in OK cells. The results are normalized to GAPDH expression, n = 6 per group, data are presented as means ± standard error.

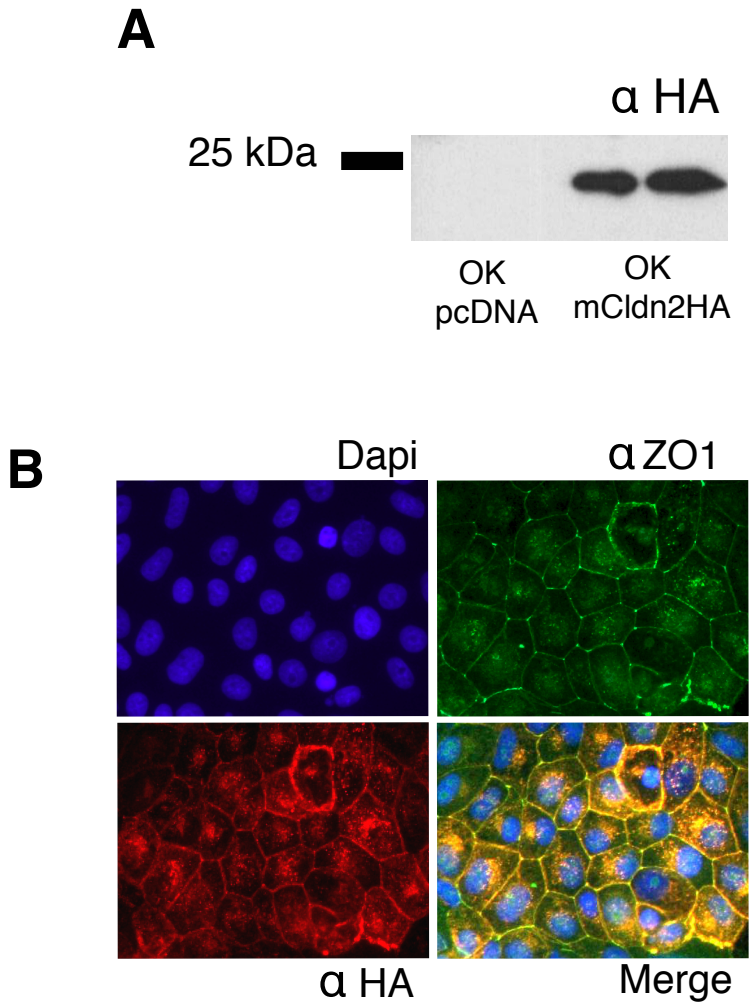

Figure 3.6 *Expression of mouse claudin-2 in OK cells.* Over-expression of claudin-2, with an HA epitope tag, in OK cells was demonstrated by western blot (A) and by immunofluorescence microscopy (B), Dapi staining is blue, ZO-1 green and claudin-2 (HA) in red.

3.3.2 Claudin-2- effects on paracellular permeability

Ussing chamber experiments utilizing OK/mClaudin-2 cells revealed a significant decrease in TER and an increase in both Na^+ and Cl^- permeability when claudin-2 was over-expressed as opposed to the empty vector (Figure 3.7 A, C&D). The pNa^+/pCl^- ratio was not significantly altered (Figure 3.7 B). Before attributing these findings solely to claudin-2 expression we first sought to study the effects of claudin-2 on the endogenous claudin levels. This is necessary because of previous reports detailing changes in endogenous claudin expression in MDCK I cells, resulting from over-expression of claudin-2 (9). Therefore, only if endogenous claudins are unaltered can the electrophysiological effect be definitively attributed to claudin-2 alone.

3.3.3 Claudin-2 expression alters endogenous claudin expression

Therefore, to ascertain whether the changes observed were due to the altered expression of claudin-2, or secondary to an effect of an alteration in other claudins, we quantified the expression of the other claudins identified in the OK cell line by qRT-PCR. The mRNA levels of claudins -1, -4, -9, -15 and -20 were unaltered in the claudin-2 over-expressing cells, compared to vector transfected controls. However, the mRNA level of claudin-12 significantly decreased and claudin-6 expression is nearly eliminated by the introduction of claudin-2 into OK cells (Figure 3.8).

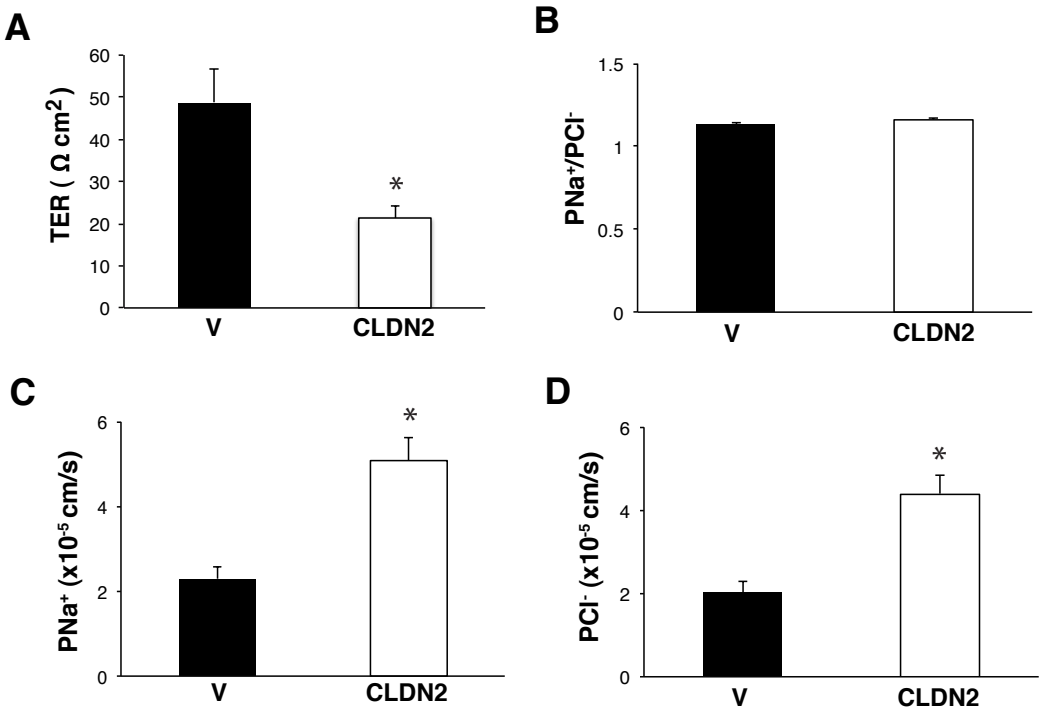

Figure 3.7 *Effects of claudin-2 expression on electrophysiology.* Ussing chamber dilution potential experiments were used to determine the TER (A), pNa^+/pCl^- (B), Na^+ (C) and Cl^- (D) permeability of cells expressing empty vector (V, black bars) or over-expressing mouse claudin-2 (CLDN2, white bars). Data are presented as means ± standard error (SE), $n \geq 3$ cell lines and * denotes a p value < 0.05.

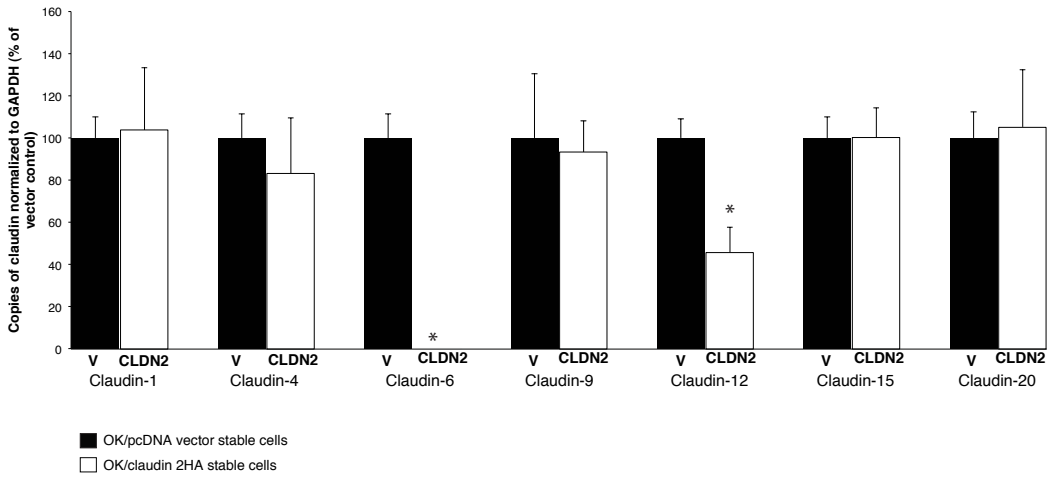

Figure 3.8 *Effects of claudin-2 over-expression on endogenous claudin expression in OK cells.* Quantitative RT-PCR analysis of claudin -1, -4, -6, -9, -12, -15 and -20 expression in OK cells expressing the empty vector (V, black bars) or claudin-2 (CLDN2, white bars). Gene expression is represented as percentage of control (OK cells stably expressing pcDNA 3.1^{+}) and normalized to the expression of GAPDH. Data are presented as means ± standard error (SE), $n \geq 3$ cell lines and * denotes a p value < 0.05.

3.4 Claudin-4

3.4.1 Claudin-4 expression and stable cell lines

We next inquired what function claudin-4, a barrier forming claudin, might play in this loose epithelial model. To this end, we cloned the endogenous opossum claudin-4 and shuttled it into the mammalian expression vector, pcDNA3.1^{+} with an HA epitope tag inserted at the carboxy terminus. Comparison between the *Didelphis virginiana* claudin-4 sequence obtained and the published *Monodelphis domestica* sequence is made in Figure 3.9. Next, we generated stable cell lines over-expressing claudin-4 to enable electrophysiological measurements on confluent monolayers. Claudin-4 over-expression was confirmed by qRT-PCR, immunoblot and immunofluorescence microscopy (Figure 3.10 A-C). Importantly, claudin-4 was predominantly localized with ZO-1 at the tight junction.

3.4.2 Claudin-4 - effects on electrophysiology

To explore the electrophysiological changes induced by claudin-4 over-expression, we performed TER and dilution potential measurements in Ussing chambers. We found that over-expression of claudin-4 in each of the individual stable cell lines caused a significant increase in TER compared to empty vector transfected OK cells (Figure 3.11A). Consistent with this, both Na^{+} and Cl^{-} permeability were significantly decreased in each of the claudin-4 over-expressing lines (Figure 3.11B&C). Moreover, the decrease in flux was reduced proportionately, such that the pNa^{+}/pCl^{-} ratio was not significantly altered (Figure 3.11 D).

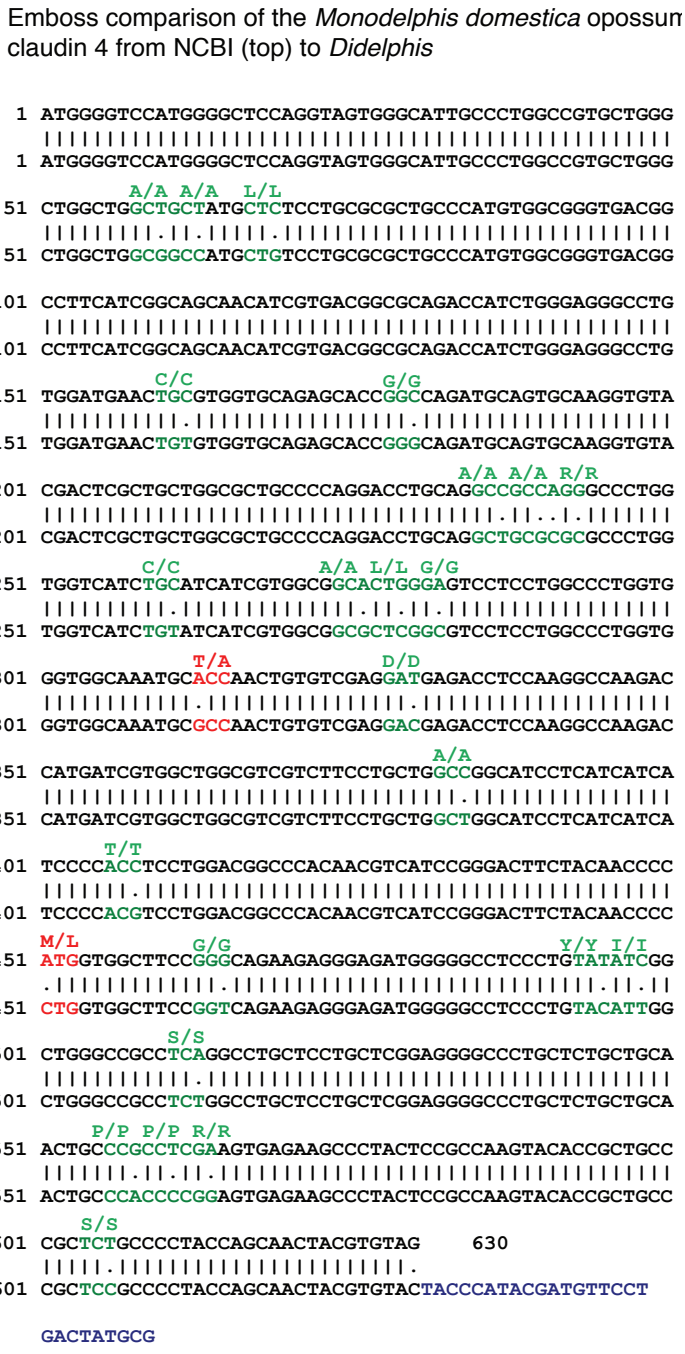

Figure 3.9 *Comparison of claudin-4 sequence between Monodelphis domestica and Didelphis virginiana opossums.* The NCBI sequence of *Monodelphis domestica* opossum claudin-4, top sequence (XM_001366871.1) was compared to the *Didelphis virginiana* opossum claudin-4, bottom sequence (obtained from the OK cell cDNA library) using Emboss Needle Pairwise Alignment software. Base pair differences coding for a synonymous amino acid are in green and non-synonymous changes are displayed in red. The coding amino acid is written above. The blue sequence at the 3' end of the *Didelphis virginiana* sequence was inserted and codes for the HA tag.

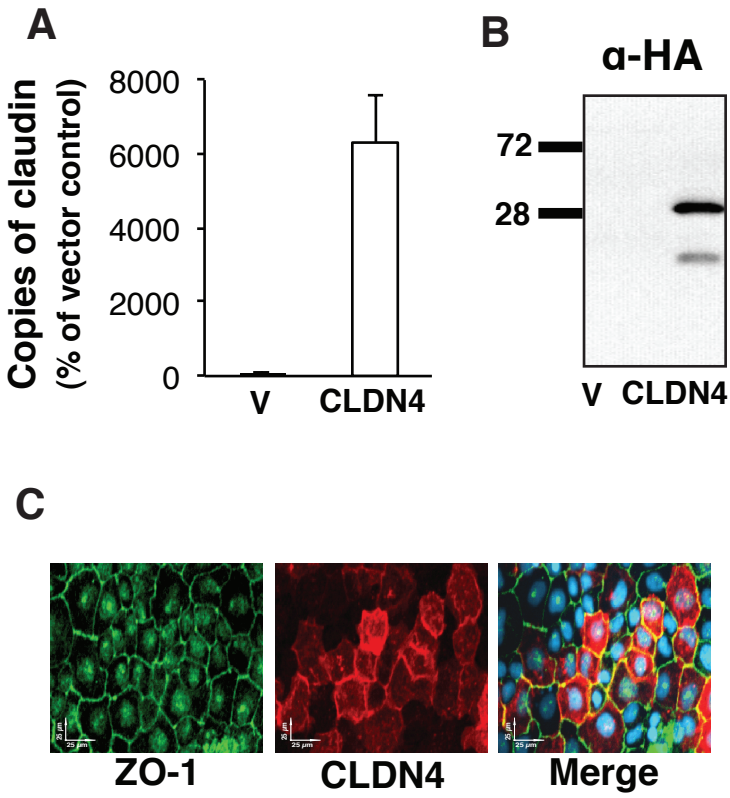

Figure 3.10 *OK cell lines stably over-expressing Claudin-4*. Claudin-4 over-expression in OK cell stable cell lines was verified by (A) qRT-PCR, presented as percentage of vector transfected control, (B) immunoblot probed for HA and (C) by immunostaining a confluent monolayer of OK cells over-expressing claudin-4HA with anti-ZO-1 (green) and anti-HA (red). OK stable cell lines over-expressing pcDNA 3.1^{+} are abbreviated V and represented with black bars, and those over-expressing claudin-4HA are represented with white bars. $n \geq 3$ cell lines for each group, data are presented as means ± standard error.

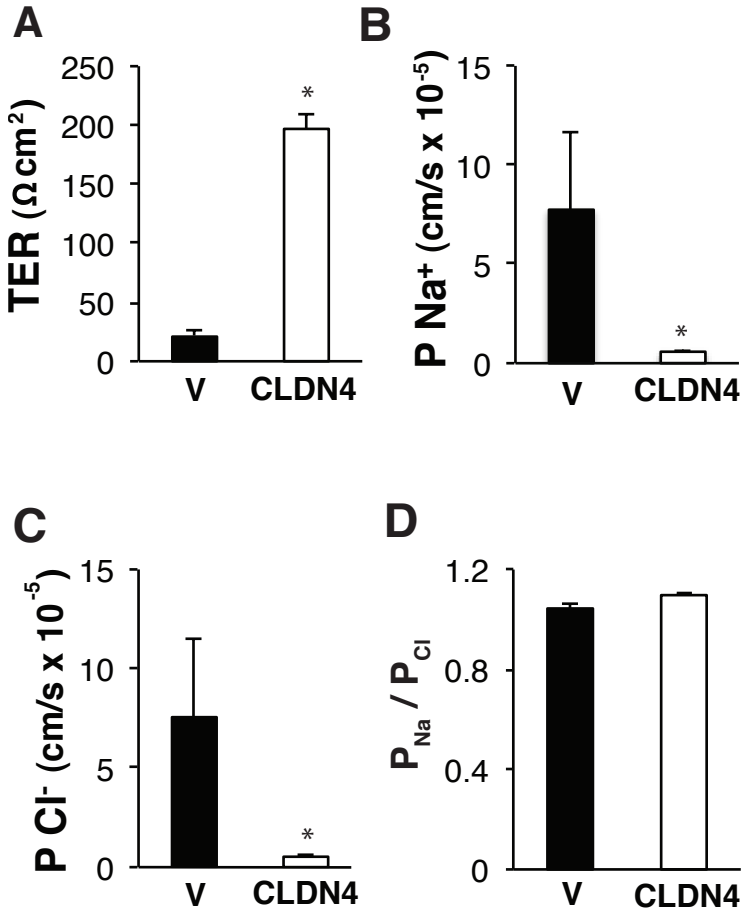

Figure 3.11 *Effects of claudin-4 expression on OK cell electrophysiology.* Ussing Chamber studies were employed to determine TER (A), absolute permeability to sodium (Na^+) (B), absolute permeability to chloride (Cl^-) (C) and the ratio of sodium to chloride permeability (pNa^+/pCl^-_1) (D). OK stable cell lines over-expressing pcDNA 3.1^+ are abbreviated V and represented with black bars, and those over-expressing claudin-4HA are represented with white bars. $n \geq 3$ cell lines for each group, data are presented as means ± standard error and * denotes a P value < 0.05.

3.4.3 Claudin-4 and paracellular flux of fluorescent dextrans

To complement our ion transport studies; we performed a fluorescent dextran flux assay using OK/pcDNA 3.1^{+} and OK/claudin-4 stable cell lines. Claudin-4 expression caused a significant increase in permeability to all three fluorescent dextrans (Figure 3.12 A-C). Consistent with its high molecular weight of 70kDa, Rhodamine B had the slowest flux rate. Of the two 3kDa dextrans, the neutral Texas Red achieved a higher flux rate than the anionic Alexa fluor 488.

3.4.4 Claudin-4- effects on endogenous claudin levels

As with claudin-2, we were aware that expression of claudin-4 might have caused perturbations in endogenous claudin expression, thereby exaggerating (or minimizing) the electrophysiological effects observed. While studying mRNA levels by qRT-PCR, we found no alteration in the expression of claudins -11, -12, -15 or -20 between empty vector expressing and claudin-4 over-expressing cell lines. However, we observed a significant increase in endogenously expressed claudins -1, -6, and -9 mRNA in the stable cell lines over-expressing exogenous claudin-4 (Figure 3.13).

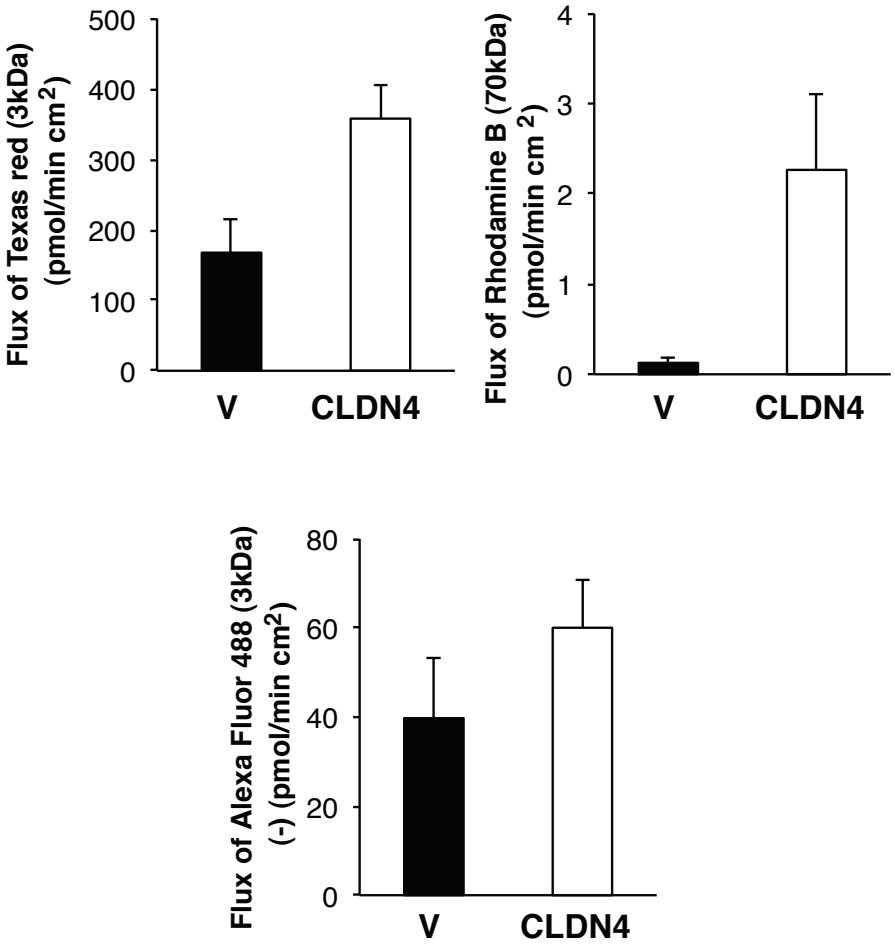

Figure 3.12 *Effects of claudin-4 on paracellular dextran flux.* The permeability to fluorescent dextrans ((A)Texas Red- 3 kDa, neutral; (B) Rhodamine B - 70 kDa, neutral, and (C) Alexa Fluor 488- 3 kDa, anionic) was determined over the course of 30 minutes across confluent monolayers of OK cells expressing pcDNA 3.1^{+} (V, black bars) or claudin-4 (CLDN4, white bars). $n \geq 3$ cell lines for each group, data are presented as means ± standard error and * denotes a P value < 0.05.

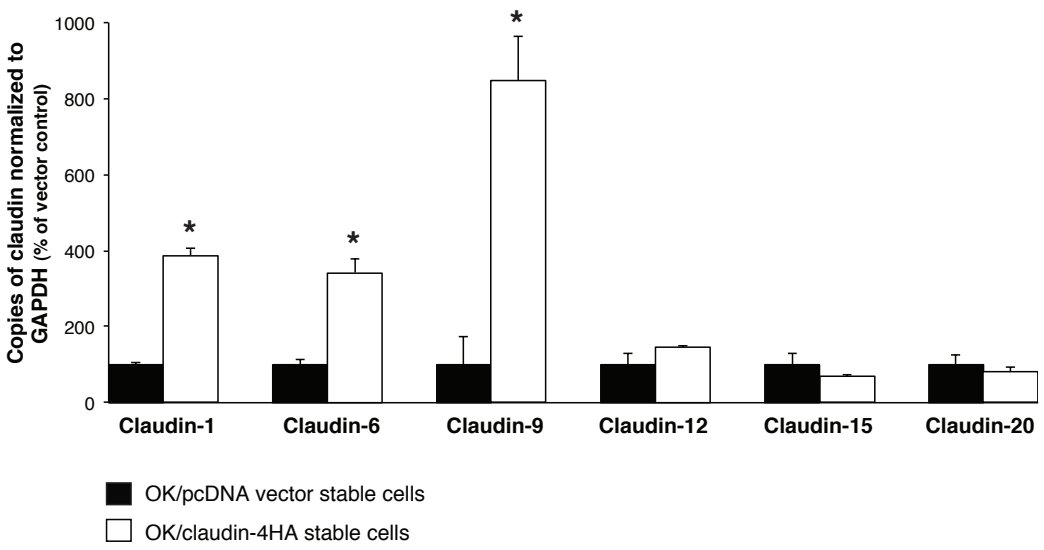

Figure 3.13 *Effects of claudin-4 over-expression on the level of expression of other claudins.* Quantitative RT-PCR analysis of claudin expression in each of the 3 OK stable cell lines expressing empty vector (black bars) or stable cell lines over-expressing claudin-4HA (n = 4). Gene expression is represented as percentage of control (OK cells stably expressing pcDNA 3.1^{+}) and normalized to the expression of GAPDH. $n \geq 3$ for each group, data are presented as means ± standard error and * denotes a P value < 0.05.

3.4.5 Claudin-4 siRNA knockdown

To more specifically dissect out the role of claudin-4 we performed siRNA knockdown of claudin-4 in OK cells as well as OK claudin-4 expressing stables (Figure 2.1). The extent of this knockdown can be visualized on the mRNA level in Figure 3.14 showing claudin-4 knockdown in OK/empty vector cells in the left panel and the claudin-4 knockdown in the OK/claudin-4 cells in the right panel. Therefore, the left panel represents a situation in which OK cells are significantly depleted of endogenous claudin-4 (by ~64%). The right panel shows knockdown of the introduced claudin-4 leading to a slight but incomplete return to endogenous levels of claudin-4 expression in OK cells. When compared to over-expression, one can expect gene knockdown to result in comparable but opposite effects on the cell physiology. Therefore, we used the claudin-4 knockdown cells to study endogenous claudin expression and electrophysiology, exactly as described before.

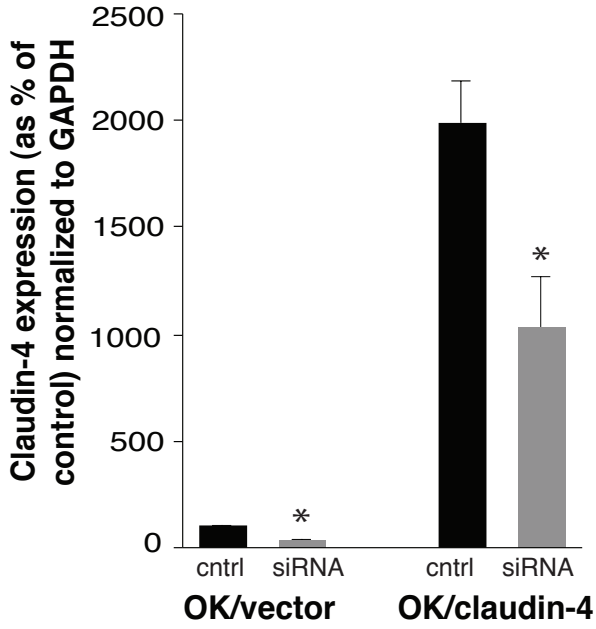

Figure 3.14 *Knockdown of endogenous and over-expressed claudin-4 in OK cells.* qRT-PCR analysis of claudin expression in empty vector expressing cells (left) and cells over-expressing claudin-4 (right) after transfection with scrambled RNA (black bars) or claudin-4 siRNA (grey bars). Gene expression is represented as percentage of control (OK cells stably expressing pcDNA 3.1^{+}) and normalized to the expression of GAPDH. Data are presented as means ± standard error (SE), $n \geq 3$ cell lines and * denotes a P value < 0.05.

Endogenous claudin-4 knockdown in OK/vector controls results in significantly decreased claudin -1, -4, -9 and -12 mRNA levels. On the other hand, the significant depletion of claudin-4 in the claudin-4 over- expressing OK cells seems to have no significant effect on the expression levels of other claudins (Figure 3.15 A-D). Therefore, much care must be taken when drawing conclusions from the results of our claudin-4 knockdown electrophysiological studies (described next). Specifically, electrophysiology of the OK endogenous claudin-4 knockdown cells represents the combined effect of claudin-4 knockdown and claudin-1, -9 and -12 down-regulation. However, claudin-4 knockdown in OK/claudin-4 cells reveals the role of claudin-4 knockdown alone (as there are no other alterations) finally making it possible to attribute the electrophysiological effects to a single claudin isoform. Ussing Chamber dilution potential studies were then used to study the electrophysiological effects of claudin-4 depletion in the OK/vector and OK/claudin-4 cells described above. There were no significant alterations in TER, absolute Na^+ or Cl^- permeability across confluent monolayers of OK cells stably expressing pcDNA 3.1^+ (the empty vector) when endogenous claudin-4 was knocked down by ~64% (Figure 3.16 A, C&D). There was a slight decrease in the pNa^+/pCl^- ratio ($p=0.04$) when the empty vector expressing cells were treated with siRNA against claudin-4 compared to scrambled siRNA (Figure 3.16 B). In contrast, the knockdown of claudin-4 in the cell lines over-expressing claudin-4 caused a significant decrease in TER, as well as a significant, proportional increase in Na^+ and Cl^- permeability, such that the pNa^+/pCl^- ratio remained unaltered (Figure 3.16 A-D).

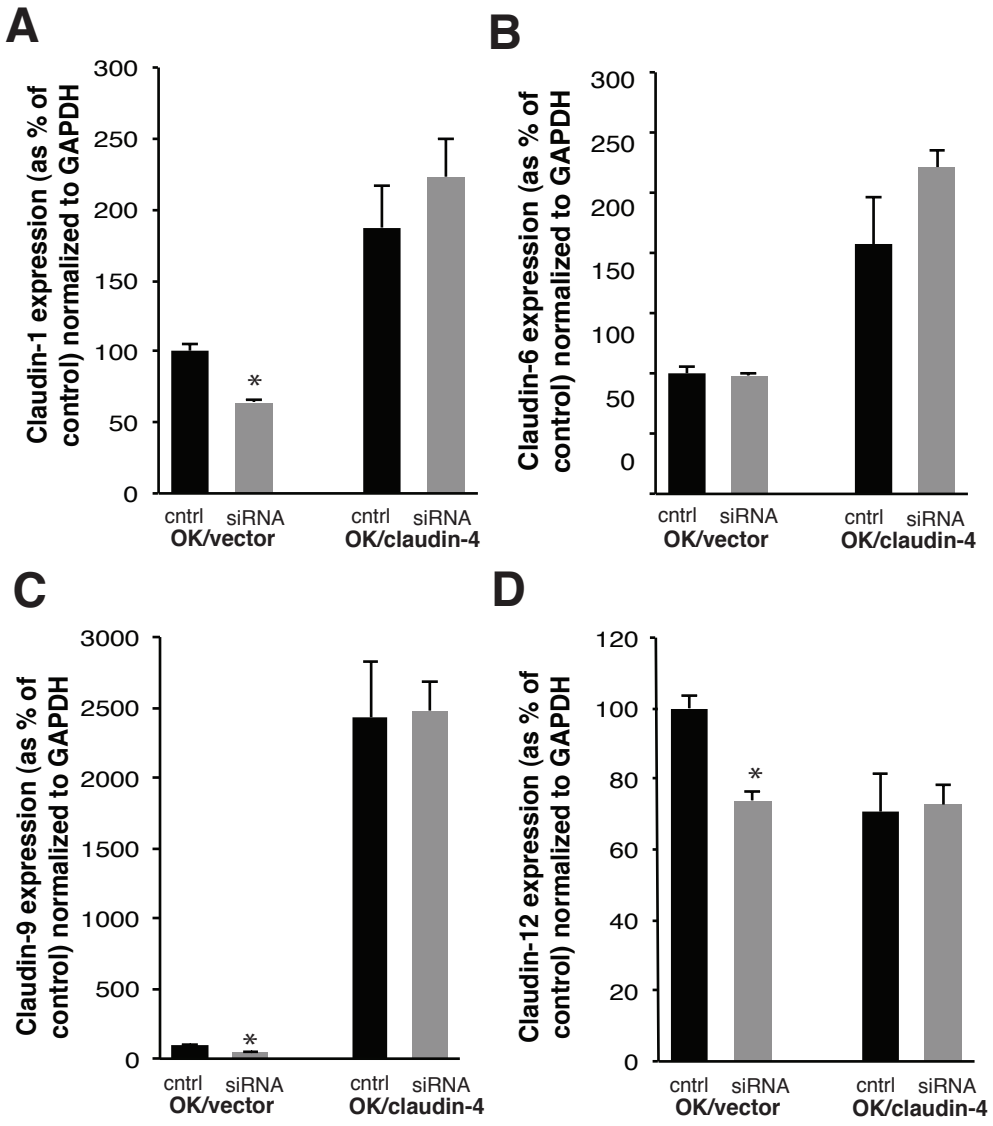

Figure 3.15 *Claudin-4 knockdown- effects on endogenous claudin expression*. qRT-PCR analysis of claudin-1 (A), -6 (B), -9 (C), and -12 (D) expression in empty vector expressing cells (left) and cells over-expressing claudin-4 (right) after transfection with scrambled RNA (black bars) or claudin-4 siRNA (grey bars). Gene expression is represented as percentage of control (OK cells stably expressing pcDNA 3.1^{+}) and normalized to the expression of GAPDH. Data are presented as means ± standard error (SE), $n \geq 3$ cell lines and * denotes a P value < 0.05.

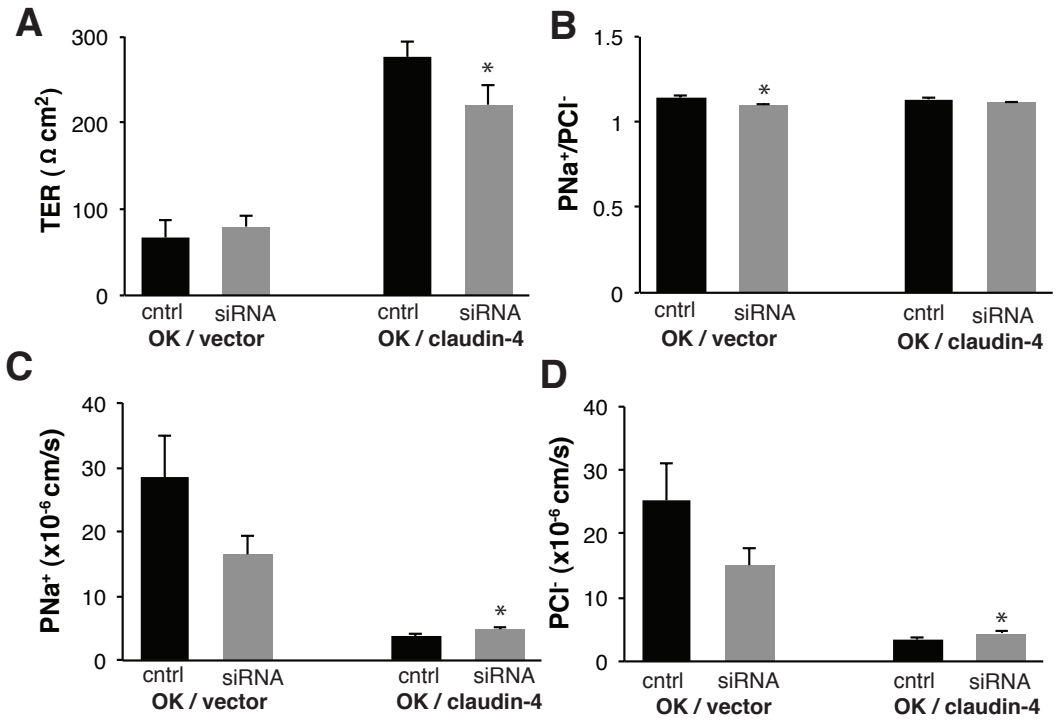

Figure 3.16 *Electrophysiological characteristics of OK claudin-4 knockdown cells.* OK cells expressing the empty vector (V) or over-expressing claudin-4 were treated for 96 hours with scrambled RNA (black bars) or claudin-4 siRNA (grey bars). Ussing chamber dilution potential experiments were then performed to determine TER (A), pNa^+/pCl^- (B) and absolute Na^+ (C) and Cl^- (D) permeability. Data are presented as means ± standard error (SE), $n \geq 3$ cell lines and * denotes a P value < 0.05.

Chapter 4

DISCUSSION

4.1 Opossum kidney cells as a model system of the proximal tubule

4.1.1 Electrophysiology

Our preliminary investigation of the opossum kidney cell line demonstrates its ability to form tight junctions (Figure 3.1). The strong linear relationship between current and voltage, as well as dilution factor and voltage, serves to justify the use of Ussing Chamber dilution potential experiments for the characterization of OK cell electrophysiology. Consequently, using these methods we determined the OK cell TER and pNa^+/pCl^- to be 11 ± 1 Ω cm^2 and 1.10 ± 0.01, respectively. These values are in strong agreement with recent *in vivo* tubular perfusion studies, which found the TER of the mouse proximal tubule (S2 segment) to be 11.3 ± 0.4 Ω cm^2 and a pNa^+/pCl^- of 1.10 ± 0.02 (77). This is also consistent with the TER measured across the proximal tubule of other species (14, 17, 64, 88, 93). The resistances of MDCK II, and LLC-PK1 cells, on the other hand, were much higher (41 ± 2 and 130 ± 5 Ω cm^2, respectively) and therefore not consistent with proximal tubule epithelium. More importantly, the selectivity of LLC-PK1 cells (pNa^+/pCl^- = 0.90 ± 0.02) and MDCK II cells (pNa^+/pCl^- = 3.2 ± 0.4) are by no means representative of the fluxes across the slightly cation selective proximal tubule. This data strongly suggests that, in terms of endogenous epithelial characteristics, OK cells better represent the proximal tubule than MDCK II cells or LLC-PK1 cells do. Furthermore, the same murine tubular perfusion studies found that K^+ was the most permeable cation followed by $Rb^+ > Na^+ > Li^+ >$ $choline^+$ (relative to Cl^-). This is identical to the permeability sequence we established for OK cells ($K^+ > Cs^+ > Rb^+ > Na^+ > Li^+$, Figure 3.3). Therefore, both

of these epithelia are associated with Eisenman sequence IV, the permeability sequence corresponding to a pore with a weak field strength binding site (32). This implies that there is a weak pore interaction permitting cations to permeate the pore largely in their hydrated state. This data emphasizes the similarity between OK cells and the PT S2 segment (77). We next asked the question whether this remarkable similarity is mirrored in the molecular composition of the tight junction as well.

4.1.2 Claudins

Claudin composition governs paracellular fluxes across the tight junction. It is, therefore surprising that claudin expression has not been completely characterized in a major site of paracellular transport like the proximal tubule. So far, claudin -2, -10, -11 (55) and -4 (83) were identified in this nephron segment. Claudin-6 and -9 were reported in the proximal tubule of neonatal (but not adult) mice (1) and the expression of claudin -12 and -20 has not yet been examined. Using two sets of degenerate PCR primers for each isoform, we have extensively characterized the claudin expression in OK cells. We identified claudin -4 > 1 > 6 > 20 > 9 > 12 > 11 and > 15 (Figures 3.4 and 3.5). Therefore, this low resistance, cation selective model expresses several supposed 'barrier forming' claudins (-1 (38, 51, 69), - 4 (104), - 6 and -9 (86)). Surprisingly the most abundant is claudin-4, an anion selective barrier forming claudin. Moreover, OK cells lack the cation selective, pore forming claudin-2. It is thought provoking to consider then, how this model system can be so loose and cation selective. Perhaps there is a strong effect induced by the proposed 'pore forming, cation selective' claudins (-12 (35)

and -15 (25, 98)), which were also found in OK cells. Likewise, the tentative contribution of claudins -11 and -20 is incalculable, as their function is still unknown. However, the claudins common to both the proximal tubule and OK cells are claudins -4, -6, -9 and potentially -11. Regardless of the discrepancies, the array of claudins expressed in OK cells form tight junctions with electrophysiological properties very similar to the proximal tubule *in vivo*. Therefore, the introduction of a "cation pore" such as claudin-2 should only exaggerate the cation selective, low resistance characteristics of the OK tight junction.

4.2 Claudin-2 in OK cells

Claudin-2 expression was observed in the proximal tubule of several species (33, 54, 83). We were therefore surprised that we could not identify it in OK cells, a proximal tubular model. However, a previous study also failed to identify claudin-2 in OK cells (81). We therefore over-expressed mouse claudin-2, and observed a decreased TER and significantly increased Na^+ and Cl^- permeability. There was a slight, but insignificant increase in the pNa^+/pCl^- ratio, suggesting that claudin-2 forms a cation selective pore in OK cells (Figure 3.7). This has been reported previously in other model systems (4, 35, 37, 104).

Somewhat to our surprise, claudin-2 overexpression also decreased claudin-12 mRNA levels and eliminated claudin-6 expression almost completely, making it impossible to ascribe the effects on permeability specifically to claudin-2 (Figure 3.8). Since we are observing these effects on the mRNA level, it is likely that claudin-2 is altering the transcription of these two isoforms. Claudin-2 could be

activating (or acting as) a repressor, which then decreases claudin-6, and -12 expression levels. Physiologically, the function of claudin-2 and -12 is similar (35), so a negative feedback mechanism might be in place to prevent robust cation permeability upon over-expression of claudin-2. In fact, it is tempting to suggest that claudin-12 plays the role of claudin-2 in OK cells (i.e. by forming a cation pore). Consequently the introduction of claudin-2 would eliminate claudin-12 because it is no longer necessary, or may make the epithelium too leaky. Claudin-6 might be responsive to the same inhibitory transcription factor, such that its expression is also eliminated.

The multiple alterations in claudin expression induced by over expressing a cation selective pore form claudin, make it difficult to ascribe the electrophysiological effects to a specific claudin isoform. As OK cells are highly permeable, and cation selective, our model system might be better suited for studying the effects of anion selective, barrier forming claudins, such as claudin-4.

4.3 Claudin-4 in OK cells

4.3.1 Claudin-4 over-expression

Of all the claudins identified in OK cells, claudin-4 is the most abundant at the level of mRNA (Figure 3.5). In the literature, claudin-4 has been classified as a cation barrier (25, 102, 104) as well as an anion channel (47). Claudin-4 knockdown leads to a TER decrease in MDCK II and increase in LLC-PK1 cells (43). From this data we can predict that claudin-4 blocks Na^+ flux in MDCK II cells and channels Cl^- in LLC-PK1 cells. In OK cells, claudin-4 expression increases TER. Therefore just like in MDCK II cells, claudin-4 may be acting as a

Na^+ barrier. Indeed, Na^+ permeability does decrease significantly upon claudin-4 expression, but Cl^- permeability does as well (Figure 3.11). As we are adding claudin-4 into an environment that is already claudin-4 rich, we may simply be overwhelming the tight junction with a barrier forming claudin, such that all ion transport is blocked.

On the other hand, we also observed higher fluorescent dextran fluxes in the claudin-4 expressing cells, compared to control (Figure 3.12). This is not consistent with claudin-4 acting as a barrier. Previous examinations of transepithelial transport mechanisms have suggested a dissociation of paracellular flux of ions from that of uncharged solutes and other macromolecules (10, 105, 107). Therefore, a change in TER might not necessarily be reflected in the permeability of uncharged solutes. In two separate studies, alterations of TER caused by claudin-2 and claudin-4 expression fail to affect the paracellualar flux of mannitol (4, 102). There seems to be one 'size restrictive high capacity pathway' through abundant small pores, and another, 'low capacity size independent pathway' through fewer much larger pores. The former pathway serves paracellular ion transport, while the latter mediates the paracellular movement of macromolecules (105, 107). This explains why increased TER was not associated with decreased flux of fluorescent dextrans in our studies. The larger, neutral 70kDa Rhodamine B dextran had the slowest flux rate, followed by the neutral 3kDa Texas Red and then anionic 3kDa Alexa Fluor 488 (Figure 3.12). Although the anionic dextran exhibits slower flux than the neutral Texas Red, this data is not inconsistent with claudin-4 being anion selective, precisely because of

the proposed second pathway of paracellular transport. Claudin-4 overexpression, however, does affect this pathway significantly, causing the "low capacity size independent" pores to become either more numerous or more permeable to dextrans upon over-expression. These results suggest the possibility of novel claudin-4 mechanisms. However, these effects may not be due to claudin-4 manipulation alone.

4.3.2 Effects on endogenous claudins

The over-expression of claudin-4 is accompanied by an increase in claudin -1, -6, and -9 mRNA (Figure 3.13). As with claudin-2, we propose these effects are carried out through alterations in transcription. Claudin-4 could be activating (or acting as) a transcription factor responsible for increased expression of the barrier forming claudin -1, -6 and -9 (51, 69, 86). In fact, claudin-1 and -4 share a common transcription factor Snail, which was observed to down-regulate these, and any other isoforms containing an E-box sequence in the promoter region (50, 67). Interestingly, one study observed up-regulation of endogenous claudin-1 resulting from the expression of any exogenous claudin isoform (113). After finding that claudin -2, -6, -7 and -9 all up-regulate claudin-1, Zavala-Zendejas *et. al.* suggest that claudin-1 expression can be regulated by numerous common transcription activators or repressors. These transcription factors are yet to be identified. There might be significant physiological relevance of claudin-4 induced up-regulation of other predicted barrier forming claudins. As the majority of ions are reabsorbed through tight junctions of the proximal tubule a physiological situation might occur that necessitates immediate tight junction

blocking. An example of this might be to prevent excessive paracellular reabsorption of sodium at times of high sodium intake. Consequently, up-regulation of an anion selective barrier forming claudin (such as claudin-4) could activate the expression of other barrier claudins (-1, -6, and -9) through common transcription factors.

It is also possible that claudins -1, -6, and -9 are potential interacting partners for claudin-4, and the over-expression of claudin-4 requires their presence in order for it to be inserted into the tight junction. More studies are needed before a conclusion can be reached regarding the mechanism of claudin-4-induced increases in claudin -1, -6, and -9 expression. One such study is the removal of claudin-4 from the tight junction by siRNA (Figure 3.14-3.16).

4.3.3 Claudin-4 knockdown

Endogenous and over-expressed claudin-4 were knocked down in OK cells and OK/claudin-4 cells, respectively. This methodology allowed us to eliminate the effects of secondary claudin up-regulation (-1, -6, and -9). Specifically, the significant knockdown of claudin-4 in the claudin-4 over-expressers did not down-regulate the levels of claudin -1, -6, and -9 (Figure 3.15, set of right panels). Therefore, the electrophysiological effect in Figure 3.16 (decreased resistance, increased sodium and chloride permeation) is due to claudin-4 knockdown alone. This data nicely complements our claudin-4 over-expression experiment, which showed an increase in resistance and decreased Na^+ and Cl^- flux. One might wonder why the expression of claudin-4 increases the levels of claudin -1, -6, and -9, but knockdown does not result in the opposite. This may be because the

OK/claudin-4 stable knockdown cells still express much more claudin-4 than wild type OK cells (~10X more claudin-4, Figure 3.14 left panel black bar *vs* right panel grey bar). The knockdown is significant when compared to the scrambled RNA control in the stable cell line, but compared to wild type OK cells, claudin-4 is still over-expressed. More importantly, this knockdown was strong enough to induce electrophysiological effects, but not strong enough to affect the regulatory mechanisms required to induce alterations in claudin -1, -6, and -9 expression. Would claudin -1, -6, and -9 be altered by knockdown of endogenous claudin-4? Figure 3.15 (left panels) illustrates a significant down-regulation of claudin -1, -9 and -12 mRNA levels upon endogenous claudin-4 knock-down, but no change in claudin-6. Therefore, the mechanism responsible for increased claudin-1 and -9 expression likely also maintains their expression in the presence of claudin-4. This correlation in expression levels is consistent with claudin-1 and -9 being interaction partners of claudin-4. However, we cannot exclude the possibility that claudin-4 is acting as (or through) a transcription factor which activates the expression of these isoforms. If this is the case, the knockdown of claudin-4 might decrease the transcription factor and consequently the levels of -1, -6 and -9. The claudin-12 expression pathway is also affected, such that claudin-12 is down-regulated as well. This could explain why we see no significant difference in the electrophysiology of OK cells and OK claudin-4 endogenous knockdown cells (Figure 3.16 A-D, left panel), with the exception of a decrease in pNa^+/pCl^-. The combined decrease of the anion selective barrier forming claudin-4 and cation selective pore forming claudin-12 could return the cells to their native

electrophysiological characteristics. There may be numerous reasons for claudin expression to cause alterations of other claudins, which is why the electrophysiological results in the literature are often inconsistent and almost always dependent on the model system employed (Section *1.5.3*) (43, 102, 104). Unfortunately, there is not enough data available to draw conclusions about the way claudins regulate each other. In fact, very few studies investigate the effects of claudin over-expression or knock-down on the levels of endogenous isoforms, often due to a lack of antibodies or other reagents. For OK cells, we have created tagged constructs and confirmed successful qRT-PCR primers and probes for each endogenous claudin isoform (Table 2.3). Therefore, OK cells have a strong advantage in being able detect delicate claudin alterations. This is a good model system of the PT where expression of claudins causes the predicted effect as well as an accompanied alteration in the endogenous claudin isoforms. In OK cells, and likely in all epithelia, claudin expression is strongly interlinked.

SUMMARY

We have characterized a very loose epithelial cell culture model and shown that it can be used to study the effect of claudins on paracellular ion transport. OK cells form tight junctions that exhibit low resistance and slight cation selectivity. We observed a linear relationship between voltage and current, as well as between the dilution factor and resulting dilution potential generated. Hence, Ussing chamber dilution potential experiments can be performed successfully on a loose epithelium. The observed electrophysiological characteristics are likely conferred by the expression of endogenous claudins, which ranks claudin-4 > -1 > -6 > -20 > -9 > -12 > -11 > -15. We employed this new model system to study the function of two different claudins: claudin-2, the cation selective "channel" claudin, and claudin-4, an anion selective barrier forming claudin. As we were unable to detect claudin-2 in this common proximal tubular cell culture model, we over-expressed mouse claudin-2 and found decreased TER, proportional increase in pNa^+ and pCl^- as well as a decrease in claudin-12 and -6 expression. On the other hand, over-expression of claudin-4 led to significantly increased TER (without altering pNa^+/pCl^-), increased permeability to fluorescent dextrans, and increased claudin-1, -6 and -9 mRNA levels. To dissect out the specific role of claudin-4 in OK cells we knocked it down in the vector transfected and the claudin-4 over-expressing cell lines. Knockdown of endogenous claudin-4 decreased claudin -1, -9, and -12 expression without significantly altering the resistance or the absolute permeability of Na^+ and Cl^-. A 64% knockdown of claudin-4 although significant, compared to scrambled RNA treated control, was not sufficient to cause

electrophysiological alterations. Obvious alterations in electrophysiology occurred only when claudin-4 was knocked down in the over-expressing stables. This did not induce significant alteration in the expression of the other endogenous claudins; allowing us to conclude that the decreased TER and increased Na^+ and Cl^- permeability are due to claudin-4. Thus, claudin-4 acts as a barrier in OK cells.

CONCLUSION

Unlike the other model systems available, OK cells closely represent the electrophysiological characteristics of the proximal tubule. However, manipulation of claudin expression in this model system significantly alters endogenous claudin expression, suggesting that claudin expression is strongly interdependent and complicating the use of this model system.

FUTURE DIRECTIONS

The claudin alterations induced by expression or knockdown were observed at the mRNA level. Since this regulation is completely unexplored, the first step is to identify the transcription factors involved and study their effects on endogenous claudins. Only then can the interdependence of claudin expression be further elucidated. It is also important to show claudin alterations at the level of protein expression, and subcellular localization. Prior to this, we must identify specific antibodies for each opossum claudin isoform. Pending the identification of specific reagents, it would be interesting to examine the possible interaction of claudins in OK cells. There seems to be a strong correlation between claudin-2 and -12, as well as claudin-4 and claudins -1, -6 & -9. By immunofluorescence, FRET and co-immunoprecipitation, it will be possible to determine whether these claudin isoforms interact. OK cells can be used in general to represent the proximal tubule, where the majority of filtered calcium is reabsorbed from. Therefore, this model system can be used to study the role of specific claudins on Ca^{2+} transport and their role in causing hypercalciuria (calcium wasting in urine).

BIBLIOGRAPHY

1. **Abuazza G, Becker A, Williams SS, Chakravarty S, Truong HT, Lin FM, and Baum M**. Claudins 6, 9, and 13 are developmentally expressed renal tight junction proteins. *Am J Physiol-Renal* 291: F1132-F1141, 2006.

2. **Akhter S, Kovbasnjuk O, Li X, Cavet M, Noel J, Arpin M, Hubbard AL, and Donowitz M**. Na^+/H^+ exchanger 3 is in large complexes in the center of the apical surface of proximal tubule-derived OK cells. *Am J Physiol-Cell Ph* 283: C927-C940, 2002.

3. **Alexandre MD, Lu Q, and Chen YH**. Overexpression of claudin-7 decreases the paracellular Cl- conductance and increases the paracellular Na^+ conductance in LLC-PK1 cells. *J Cell Sci* 118: 2683-2693, 2005.

4. **Amasheh S, Meiri N, Gitter AH, Schoneberg T, Mankertz J, Schulzke JD, and Fromm M**. Claudin-2 expression induces cation-selective channels in tight junctions of epithelial cells. *J Cell Sci* 115: 4969-4976, 2002.

5. **Amemiya M, Loffing J, Lotscher M, Kaissling B, Alpern RJ, and Moe OW**. Expression of Nhe-3 in the Apical Membrane of Rat Renal Proximal Tubule and Thick Ascending Limb. *Kidney Int* 48: 1206-1215, 1995.

6. **Amemiya M, Yamaji Y, Cano A, Moe OW, and Alpern RJ**. Acid Incubation Increases Nhe-3 Messenger-Rna Abundance in Okp Cells. *Am J Physiol-Cell Ph* 269: C126-C133, 1995.

7. **Anderson JM, and Van Itallie CM**. Physiology and function of the tight junction. *Cold Spring Harb Perspect Biol* 1: a002584, 2009.

8. **Angelow S, El-Husseini R, Kanzawa SA, and Yu ASL**. Renal localization and function of the tight junction protein, claudin-19. *Am J Physiol-Renal* 293: F166-F177, 2007.

9. **Angelow S, Schneeberger EE, and Yu AS**. Claudin-8 expression in renal epithelial cells augments the paracellular barrier by replacing endogenous claudin-2. *J Membr Biol* 215: 147-159, 2007.

10. **Balda MS, Whitney JA, Flores C, Gonzalez S, Cereijido M, and Matter K**. Functional dissociation of paracellular permeability and transepithelial electrical resistance and disruption of the apical-basolateral intramembrane diffusion barrier by expression of a mutant tight junction membrane protein. *Mol Biol Cell* 7: 3534-3534, 1996.

11. **Balkovetz DF**. Claudins at the gate: determinants of renal epithelial tight junction paracellular permeability. *Am J Physiol-Renal* 290: F572-F579, 2006.

12. **Barker G, and Simmons NL**. Identification of two strains of cultured canine renal epithelial cells (MDCK cells) which display entirely different physiological properties. *Q J Exp Physiol* 66: 61-72, 1981.

13. **Baum M, and Quigley R**. Maturation of rat proximal tubule chloride permeability. *Am J Physiol-Reg I* 289: R1659-R1664, 2005.

14. **Bello-Reuss E**. Cell membranes and paracellular resistances in isolated renal proximal tubules from rabbit and Ambystoma. *J Physiol* 370: 25-38, 1986.

15. **Ben-Yosef T, Belyantseva IA, Saunders TL, Hughes ED, Kawamoto K, Van Itallie CM, Beyer LA, Halsey K, Gardner DJ, Wilcox ER, Rasmussen J, Anderson JM, Dolan DF, Forge A, Raphael Y, Camper SA, and Friedman TB**. Claudin 14 knockout mice, a model for autosomal recessive deafness DFNB29, are deaf due to cochlear hair cell degeneration. *Hum Mol Genet* 12: 2049-2061, 2003.

16. **Boron WF**. Acid-base transport by the renal proximal tubule. *J Am Soc Nephrol* 17: 2368-2382, 2006.

17. **Boulpaep EL, and Seely JF**. Electrophysiology of proximal and distal tubules in the autoperfused dog kidney. *Am J Physiol* 221: 1084-1096, 1971.

18. **Boutet A, De Frutos CA, Maxwell PH, Mayol MJ, Romero J, and Nieto MA**. Snail activation disrupts tissue homeostasis and induces fibrosis in the adult kidney. *Embo J* 25: 5603-5613, 2006.

19. **Cano A, Perez-Moreno MA, Rodrigo I, Locascio A, Blanco MJ, del Barrio MG, Portillo F, and Nieto MA**. The transcription factor Snail controls epithelial-mesenchymal transitions by repressing E-cadherin expression. *Nat Cell Biol* 2: 76-83, 2000.

20. **Carpi-Medina P, and Whittembury G**. Comparison of transcellular and transepithelial water osmotic permeabilities (Pos) in the isolated proximal straight tubule (PST) of the rabbit kidney. *Pflugers Arch* 412: 66-74, 1988.

21. **Carrozzino F, Soulie P, Huber D, Mensi N, Orci L, Cano A, Feraille E, and Montesano R**. Inducible expression of Snail selectively increases paracellular ion permeability and differentially modulates tight junction proteins. *Am J Physiol Cell Physiol* 289: C1002-1014, 2005.

22. **Claude P**. Morphological factors influencing transepithelial permeability: a model for the resistance of the zonula occludens. *J Membr Biol* 39: 219-232, 1978.

23. **Claude P, and Goodenough DA**. Fracture faces of zonulae occludentes from "tight" and "leaky" epithelia. *The Journal of cell biology* 58: 390-400, 1973.

24. **Colegio OR, Van Itallie C, Rahner C, and Anderson JM**. Claudin extracellular domains determine paracellular charge selectivity and resistance but not tight junction fibril architecture. *Am J Physiol Cell Physiol* 284: C1346-1354, 2003.

25. **Colegio OR, Van Itallie CM, McCrea HJ, Rahner C, and Anderson JM**. Claudins create charge-selective channels in the paracellular pathway between epithelial cells. *Am J Physiol-Cell Ph* 283: C142-C147, 2002.

26. **Corman B, Roinel N, and De Rouffignac C**. Water reabsorption capacity of the proximal convoluted tubule: a microperfusion study on rat kidney. *J Physiol* 316: 379-392, 1981.

27. **Coyne CB, Gambling TM, Boucher RC, Carson JL, and Johnson LG**. Role of claudin interactions in airway tight junctional permeability. *Am J Physiol Lung Cell Mol Physiol* 285: L1166-1178, 2003.

28. **Daugherty BL, Ward C, Smith T, Ritzenthaler JD, and Koval M**. Regulation of heterotypic claudin compatibility. *J Biol Chem* 282: 30005-30013, 2007.

29. **De Craene B, Gilbert B, Stove C, Bruyneel E, van Roy F, and Berx G**. The transcription factor snail induces tumor cell invasion through modulation of the epithelial cell differentiation program. *Cancer Res* 65: 6237-6244, 2005.

30. **Dukes JD, Whitley P, and Chalmers AD**. The MDCK variety pack: choosing the right strain. *Bmc Cell Biol* 12: 2011.

31. **Earley LE, Martino JA, and Friedler RM**. Factors affecting sodium reabsorption by the proximal tubule as determined during blockade of distal sodium reabsorption. *J Clin Invest* 45: 1668-1684, 1966.

32. **Eisenman G, and Horn R**. Ionic selectivity revisited: the role of kinetic and equilibrium processes in ion permeation through channels. *J Membr Biol* 76: 197-225, 1983.

33. **Enck AH, Berger UV, and Yu ASL**. Claudin-2 is selectively expressed in proximal nephron in mouse kidney. *Am J Physiol-Renal* 281: F966-F974, 2001.

34. **Escaffit F, Boudreau F, and Beaulieu JF**. Differential expression of claudin-2 along the human intestine: Implication of GATA-4 in the maintenance of claudin-2 in differentiating cells. *J Cell Physiol* 203: 15-26, 2005.

35. **Fujita H, Sugimoto K, Inatomi S, Maeda T, Osanai M, Uchiyama Y, Yamamoto Y, Wada T, Kojima T, Yokozaki H, Yamashita T, Kato S, Sawada N, and Chiba H**. Tight junction proteins claudin-2 and -12 are critical for vitamin D-dependent Ca^{2+} absorption between enterocytes. *Mol Biol Cell* 19: 1912-1921, 2008.

36. **Furuse M, Fujita K, Hiiragi T, Fujimoto K, and Tsukita S**. Claudin-1 and -2: Novel integral membrane proteins localizing at tight junctions with no sequence similarity to occludin. *J Cell Biol* 141: 1539-1550, 1998.

37. **Furuse M, Furuse K, Sasaki H, and Tsukita S**. Conversion of Zonulae occludentes from tight to leaky strand type by introducing claudin-2 into Madin-Darby canine kidney I cells. *J Cell Biol* 153: 263-272, 2001.

38. **Furuse M, Hata M, Furuse K, Yoshida Y, Haratake A, Sugitani Y, Noda T, Kubo A, and Tsukita S**. Claudin-based tight junctions are crucial for the mammalian epidermal barrier: a lesson from claudin-1-deficient mice. *J Cell Biol* 156: 1099-1111, 2002.

39. **Furuse M, Sasaki H, Fujimoto K, and Tsukita S**. A single gene product, claudin-1 or -2, reconstitutes tight junction strands and recruits occludin in fibroblasts. *The Journal of cell biology* 143: 391-401, 1998.

40. **Furuse M, Sasaki H, and Tsukita S**. Manner of interaction of heterogeneous claudin species within and between tight junction strands. *The Journal of cell biology* 147: 891-903, 1999.

41. **Giebisch G**. Renal potassium transport: mechanisms and regulation. *Am J Physiol* 274: F817-833, 1998.

42. **Hoenderop JG, Nilius B, and Bindels RJ**. Calcium absorption across epithelia. *Physiol Rev* 85: 373-422, 2005.

43. **Hou J, Gomes AS, Paul DL, and Goodenough DA**. Study of claudin function by RNA interference. *J Biol Chem* 281: 36117-36123, 2006.

44. **Hou JH, Paul DL, and Goodenough DA**. Paracellin-1 and the modulation of ion selectivity of tight junctions. *J Cell Sci* 118: 5109-5118, 2005.

45. **Hou JH, Renigunta A, Gomes AS, Hou ML, Paul DL, Waldegger S, and Goodenough DA**. Claudin-16 and claudin-19 interaction is required for their assembly into tight junctions and for renal reabsorption of magnesium. *Proc Natl Acad Sci U S A* 106: 15350-15355, 2009.

46. **Hou JH, Renigunta A, Konrad M, Gornes AS, Schneeberger EE, Paul DL, Waldegger S, and Goodenough DA**. Claudin-16 and claudin-19 interact and form a cation-selective tight junction complex. *Journal of Clinical Investigation* 118: 619-628, 2008.

47. **Hou JH, Renigunta A, Yang J, and Waldegger S**. Claudin-4 forms paracellular chloride channel in the kidney and requires claudin-8 for tight junction localization. *Proc Natl Acad Sci U S A* 107: 18010-18015, 2010.

48. **Hull RN, Cherry WR, and Weaver GW**. The origin and characteristics of a pig kidney cell strain, LLC-PK. *In Vitro* 12: 670-677, 1976.

49. **Ikari A, Hirai N, Shiroma M, Harada H, Sakai H, Hayashi H, Suzuki Y, Degawa M, and Takagi K**. Association of paracellin-1 with ZO-1 augments the reabsorption of divalent cations in renal epithelial cells. *J Biol Chem* 279: 54826-54832, 2004.

50. **Ikenouchi J, Matsuda M, Furuse M, and Tsukita S**. Regulation of tight junctions during the epithelium-mesenchyme transition: direct repression of the gene expression of claudins/occludin by Snail. *J Cell Sci* 116: 1959-1967, 2003.

51. **Inai T, Kobayashi J, and Shibata Y**. Claudin-1 contributes to the epithelial barrier function in MDCK cells. *Eur J Cell Biol* 78: 849-855, 1999.

52. **Jaumouille V, Krishnan D, and Alexander RT**. The calmodulin antagonist W-7 inhibits the epithelial Na^+/H^+ exchanger via modulating membrane surface potential. *Channels (Austin)* 5: 308-313, 2011.

53. **Kimizuka H, and Koketsu K**. Ion Transport through Cell Membrane. *J Theor Biol* 6: 290-&, 1964.

54. **Kirk A, Campbell S, Bass P, Mason J, and Collins J**. Differential expression of claudin tight junction proteins in the human cortical nephron. *Nephrol Dial Transpl* 25: 2107-2119, 2010.

55. **Kiuchi-Saishin Y, Gotoh S, Furuse M, Takasuga A, Tano Y, and Tsukita S**. Differential expression patterns of claudins, tight junction membrane proteins, in mouse nephron segments. *Journal of the American Society of Nephrology* 13: 2002.

56. **Koeppen BaSB**. *Renal Physiology*. 2007.

57. **Koyama H, Goodpasture C, Miller MM, Teplitz RL, and Riggs AD**. Establishment and characterization of a cell line from the American opossum (Didelphys virginiana). *In Vitro* 14: 239-246, 1978.

58. **Kozak M**. An analysis of 5'-noncoding sequences from 699 vertebrate messenger RNAs. *Nucleic Acids Res* 15: 8125-8148, 1987.

59. **Krause G, Winkler L, Mueller SL, Haseloff RF, Piontek J, and Blasig IE**. Structure and function of claudins. *Biochim Biophys Acta* 1778: 631-645, 2008.

60. **Krug SM, Gunzel D, Conrad MP, Lee IF, Amasheh S, Fromm M, and Yu AS**. Charge-selective claudin channels. *Ann N Y Acad Sci* 1257: 20-28, 2012.

61. **Lee WK, Torchalski B, Kohistani N, and Thevenod F**. ABCB1 protects kidney proximal tubule cells against cadmium-induced apoptosis: roles of cadmium and ceramide transport. *Toxicol Sci* 121: 343-356, 2011.

62. **Lewis SA, Eaton DC, and Diamond JM**. The mechanism of Na^+ transport by rabbit urinary bladder. *J Membr Biol* 28: 41-70, 1976.

63. **Liang M, Ramsey CR, and Knox FG**. The paracellular permeability of opossum kidney cells, a proximal tubule cell line. *Kidney Int* 56: 2304-2308, 1999.

64. **Lutz MD, Cardinal J, and Burg MB**. Electrical resistance of renal proximal tubule perfused in vitro. *Am J Physiol* 225: 729-734, 1973.

65. **Maddox DA, and Gennari FJ**. The early proximal tubule: a high-capacity delivery-responsive reabsorptive site. *Am J Physiol* 252: F573-584, 1987.

66. **Madin SH, Andriese PC, and Darby NB**. The in vitro cultivation of tissues of domestic and laboratory animals. *Am J Vet Res* 18: 932-941, 1957.

67. **Martinez-Estrada OM, Culleres S, Soriano FX, Peinado H, Bolos V, Martinez FO, Reina M, Cano A, Fabre M, and Vilaro S**. The transcription

factors Slug and Snail act as repressors of Claudin-1 expression in epithelial cells. *Biochemical Journal* 394: 449-457, 2006.

68. **Matsuda M, Kubo A, Furuse M, and Tsukita S**. A peculiar internalization of claudins, tight junction-specific adhesion molecules, during the intercellular movement of epithelial cells. *J Cell Sci* 117: 1247-1257, 2004.

69. **McCarthy KM, Francis SA, McCormack JM, Lai J, Rogers RA, Skare IB, Lynch RD, and Schneeberger EE**. Inducible expression of claudin-1-myc but not occludin-VSV-G results in aberrant tight junction strand formation in MDCK cells. *J Cell Sci* 113: 3387-3398, 2000.

70. **Mendes F, Wakefield J, Bachhuber T, Barroso M, Bebok Z, Penque D, Kunzelmann K, and Amaral MD**. Establishment and characterization of a novel polarized MDCK epithelial cellular model for CFTR studies. *Cell Physiol Biochem* 16: 281-290, 2005.

71. **Mikkelsen TS, Wakefield MJ, Aken B, Amemiya CT, Chang JL, Duke S, Garber M, Gentles AJ, Goodstadt L, Heger A, Jurka J, Kamal M, Mauceli E, Searle SM, Sharpe T, Baker ML, Batzer MA, Benos PV, Belov K, Clamp M, Cook A, Cuff J, Das R, Davidow L, Deakin JE, Fazzari MJ, Glass JL, Grabherr M, Greally JM, Gu W, Hore TA, Huttley GA, Kleber M, Jirtle RL, Koina E, Lee JT, Mahony S, Marra MA, Miller RD, Nicholls RD, Oda M, Papenfuss AT, Parra ZE, Pollock DD, Ray DA, Schein JE, Speed TP, Thompson K, VandeBerg JL, Wade CM, Walker JA, Waters PD, Webber C, Weidman JR, Xie X, Zody MC, Graves JA, Ponting CP, Breen M, Samollow PB, Lander ES, and Lindblad-Toh K**. Genome of the marsupial Monodelphis domestica reveals innovation in non-coding sequences. *Nature* 447: 167-177, 2007.

72. **Mineta K, Yamamoto Y, Yamazaki Y, Tanaka H, Tada Y, Saito K, Tamura A, Igarashi M, Endo T, Takeuchi K, and Tsukita S**. Predicted expansion of the claudin multigene family. *FEBS Lett* 585: 606-612, 2011.

73. **Misfeldt DS, Hamamoto ST, and Pitelka DR**. Transepithelial transport in cell culture. *Proc Natl Acad Sci U S A* 73: 1212-1216, 1976.

74. **Mitic LL, Unger VM, and Anderson JM**. Expression, solubilization, and biochemical characterization of the tight junction transmembrane protein claudin-4. *Protein Sci* 12: 218-227, 2003.

75. **Mitic LL, Van Itallie CM, and Anderson JM**. Molecular physiology and pathophysiology of tight junctions I. Tight junction structure and function: lessons from mutant animals and proteins. *Am J Physiol Gastrointest Liver Physiol* 279: G250-254, 2000.

76. **Murer H, Hernando N, Forster I, and Biber J**. Proximal tubular phosphate reabsorption: molecular mechanisms. *Physiol Rev* 80: 1373-1409, 2000.

77. **Muto S, Hata M, Taniguchi J, Tsuruoka S, Moriwaki K, Saitou M, Furuse K, Sasaki H, Fujimura A, Imai M, Kusano E, Tsukita S, and Furuse M**. Claudin-2-deficient mice are defective in the leaky and cation-selective paracellular permeability properties of renal proximal tubules. *Proc Natl Acad Sci U S A* 107: 8011-8016, 2010.

78. **Niimi T, Nagashima K, Ward JM, Minoo P, Zimonjic DB, Popescu NC, and Kimura S**. claudin-18, a novel downstream target gene for the T/EBP/NKX2.1 homeodomain transcription factor, encodes lung- and stomach-specific isoforms through alternative splicing. *Mol Cell Biol* 21: 7380-7390, 2001.

79. **Ohkubo T, and Ozawa M**. The transcription factor Snail downregulates the tight junction components independently of E-cadherin downregulation. *J Cell Sci* 117: 1675-1685, 2004.

80. **Piontek J, Winkler L, Wolburg H, Muller SL, Zuleger N, Piehl C, Wiesner B, Krause G, and Blasig IE**. Formation of tight junction: determinants of homophilic interaction between classic claudins. *Faseb J* 22: 146-158, 2008.

81. **Prozialeck WC, Edwards JR, Lamar PC, and Smith CS**. Epithelial barrier characteristics and expression of cell adhesion molecules in proximal tubule-derived cell lines commonly used for in vitro toxicity studies. *Toxicol In Vitro* 20: 942-953, 2006.

82. **Rabito CA**. Occluding junctions in a renal cell line (LLC-PK1) with characteristics of proximal tubular cells. *Am J Physiol* 250: F734-743, 1986.

83. **Reyes JL, Lamas M, Martin D, Namorado MD, Islas S, Luna J, Tauc M, and Gonzalez-Mariscal L**. The renal segmental distribution of claudins changes with development. *Kidney Int* 62: 476-487, 2002.

84. **Richardson JC, Scalera V, and Simmons NL**. Identification of two strains of MDCK cells which resemble separate nephron tubule segments. *Biochim Biophys Acta* 673: 26-36, 1981.

85. **Rosenthal R, Milatz S, Krug SM, Oelrich B, Schulzke JD, Amasheh S, Gunzel D, and Fromm M**. Claudin-2, a component of the tight junction, forms a paracellular water channel. *J Cell Sci* 123: 1913-1921, 2010.

86. **Sas D, Hu M, Moe OW, and Baum M**. Effect of claudins 6 and 9 on paracellular permeability in MDCK II cells. *Am J Physiol Regul Integr Comp Physiol* 295: R1713-1719, 2008.

87. **Satake S, Semba S, Matsuda Y, Usami Y, Chiba H, Sawada N, Kasuga M, and Yokozaki H**. Cdx2 transcription factor regulates claudin-3 and claudin-4 expression during intestinal differentiation of gastric carcinoma. *Pathol Int* 58: 156-163, 2008.

88. **Schafer JA, Troutman SL, and Andreoli TE**. Volume reabsorption, transepithelial potential differences, and ionic permeability properties in mammalian superficial proximal straight tubules. *J Gen Physiol* 64: 582-607, 1974.

89. **Schepers MS, Duim RA, Asselman M, Romijn JC, Schroder FH, and Verkoelen CF**. Internalization of calcium oxalate crystals by renal tubular cells: a nephron segment-specific process? *Kidney Int* 64: 493-500, 2003.

90. **Schepers MS, van Ballegooijen ES, Bangma CH, and Verkoelen CF**. Crystals cause acute necrotic cell death in renal proximal tubule cells, but not in collecting tubule cells. *Kidney Int* 68: 1543-1553, 2005.

91. **Schild L, Giebisch G, and Green R**. Chloride transport in the proximal renal tubule. *Annu Rev Physiol* 50: 97-110, 1988.

92. **Schwegler JS, Heuner A, and Silbernagl S**. Electrical properties of cultured renal tubular cells (OK) grown in confluent monolayers. *Pflugers Arch* 415: 183-190, 1989.

93. **Seely JF**. Variation in electrical resistance along length of rat proximal convoluted tubule. *Am J Physiol* 225: 48-57, 1973.

94. **Shen L, Weber CR, Raleigh DR, Yu D, and Tumer JR**. Tight, Junction Pore and Leak Pathways: A Dynamic Duo. *Annual Review of Physiology, Vol 73* 283-309, 2011.

95. **Singh AB, Sugimoto K, Dhawan P, and Harris RC**. Juxtacrine activation of EGFR regulates claudin expression and increases transepithelial resistance. *Am J Physiol-Cell Ph* 293: C1660-C1668, 2007.

96. **Sonoda N, Furuse M, Sasaki H, Yonemura S, Katahira J, Horiguchi Y, and Tsukita S**. Clostridium perfringens enterotoxin fragment removes specific claudins from tight junction strands: Evidence for direct involvement of claudins in tight junction barrier. *The Journal of cell biology* 147: 195-204, 1999.

97. **Svennevig K, Prydz K, and Kolset SO**. Proteoglycans in polarized epithelial Madin-Darby canine kidney cells. *Biochem J* 311 (Pt 3): 881-888, 1995.

98. **Tamura A, Hayashi H, Imasato M, Yamazaki Y, Hagiwara A, Wada M, Noda T, Watanabe M, Suzuki Y, and Tsukita S**. Loss of claudin-15, but not claudin-2, causes Na^+ deficiency and glucose malabsorption in mouse small intestine. *Gastroenterology* 140: 913-923, 2011.

99. **Tang VW, and Goodenough DA**. Paracellular ion channel at the tight junction. *Biophys J* 84: 1660-1673, 2003.

100. **Tsukita S, Furuse M, and Itoh M**. Multifunctional strands in tight junctions. *Nat Rev Mol Cell Biol* 2: 285-293, 2001.

101. **Umeda K, Ikenouchi J, Katahira-Tayama S, Furuse K, Sasaki H, Nakayama M, Matsui T, Tsukita S, Furuse M, and Tsukita S**. ZO-1 and ZO-2 independently determine where claudins are polymerized in tight-junction strand formation. *Cell* 126: 741-754, 2006.

102. **Van Itallie C, Rahner C, and Anderson JM**. Regulated expression of claudin-4 decreases paracellular conductance through a selective decrease in sodium permeability. *Journal of Clinical Investigation* 107: 1319-1327, 2001.

103. **Van Itallie CM, and Anderson JM**. Claudins and epithelial paracellular transport. *Annu Rev Physiol* 68: 403-429, 2006.

104. **Van Itallie CM, Fanning AS, and Anderson JM**. Reversal of charge selectivity in cation or anion-selective epithelial lines by expression of different claudins. *Am J Physiol Renal Physiol* 285: F1078-1084, 2003.

105. **Van Itallie CM, Holmes J, Bridges A, Gookin JL, Coccaro MR, Proctor W, Colegio OR, and Anderson JM**. The density of small tight junction pores varies among cell types and is increased by expression of claudin-2. *J Cell Sci* 121: 298-305, 2008.

106. **Van Itallie CM, Rogan S, Yu A, Vidal LS, Holmes J, and Anderson JM**. Two splice variants of claudin-10 in the kidney create paracellular pores with different ion selectivities. *Am J Physiol-Renal* 291: F1288-F1299, 2006.

107. **Watson CJ, Rowland M, and Warhurst G**. Functional modeling of tight junctions in intestinal cell monolayers using polyethylene glycol oligomers. *Am J Physiol-Cell Ph* 281: C388-C397, 2001.

108. **Wen HJ, Watry DD, Marcondes MCG, and Fox HS**. Selective decrease in paracellular conductance of tight junctions: role of the first extracellular domain of claudin-5. *Mol Cell Biol* 24: 8408-8417, 2004.

109. **Widmaier EP HRaSK**. *Vander, Sherman and Luciano's Human Physiology*. 2004.

110. **Yu A**. Claudins. In: *Current Topics in Membranes*Elsevier, 2010, p. 39-78.

111. **Yu AS, Enck AH, Lencer WI, and Schneeberger EE**. Claudin-8 expression in Madin-Darby canine kidney cells augments the paracellular barrier to cation permeation. *J Biol Chem* 278: 17350-17359, 2003.

112. **Yu ASL, Cheng MH, Angelow S, Gunzel D, Kanzawa SA, Schneeberger EE, Fromm M, and Coalson RD**. Molecular Basis for Cation Selectivity in Claudin-2-based Paracellular Pores: Identification of an Electrostatic Interaction Site. *Journal of General Physiology* 133: 111-127, 2009.

113. **Zavala-Zendejas VE, Torres-Martinez AC, Salas-Morales B, Fortoul TI, Montano LF, and Rendon-Huerta EP**. Claudin-6, 7, or 9 overexpression in the human gastric adenocarcinoma cell line AGS increases its invasiveness, migration, and proliferation rate. *Cancer Invest* 29: 1-11, 2011.